AD-A216 671

(4)

College of Earth and Mineral Sciences

PENNSTATE

1855

ANNUAL REPORT

to

OFFICE OF NAVAL RESEARCH

Contract USN 00014-84-K-0201

January 1990

A REVIEW OF THE
MECHANISM AND KINETICS OF ELECTROCHEMICAL HYDROGEN ENTRY AND
DEGRADATION OF METALLIC SYSTEMS

H. W. Pickering

Department of Materials Science and Engineering
The Pennsylvania State University

90 01 09 176

PENN STATE
College of Earth and
Mineral Sciences

Undergraduate Majors

Ceramic Science and Engineering, Fuel Science, Metals Science and Engineering, Polymer Science;
Mineral Economics; Mining Engineering, Petroleum and Natural Gas Engineering;
Earth Sciences, Geosciences; Geography; Meteorology.

Graduate Programs and Fields of Research

Ceramic Science and Engineering, Fuel Science, Metals Science and Engineering, Polymer Science;
Mineral Economics; Mining Engineering, Mineral Processing, Petroleum and Natural Gas
Engineering;
Geochemistry and Mineralogy, Geology, Geophysics; Geography; Meteorology.

Universitywide Interdisciplinary Graduate Programs Involving EMS Faculty and Students

Earth Sciences, Ecology, Environmental Pollution Control Engineering, Mineral Engineering
Management, Solid State Science.

Associate Degree Programs

Metallurgical Engineering Technology (Shenango Valley Campus).

Interdisciplinary Research Groups Centered in the College

C. Drew Stahl Center for Advanced Oil Recovery, Center for Advanced Materials, Coal Research
Section, Earth System Science Center, Mining and Mineral Resources Research Institute, Ore
Deposits Research Group.

Analytical and Characterization Laboratories (Mineral Constitution Laboratories)

Services available include: classical chemical analysis of metals and silicate and carbonate rocks;
X-ray diffraction and fluorescence; electron microscopy and diffraction; electron microprobe
analysis; atomic absorption analysis; spectrochemical analysis; surface analysis by secondary ion
mass spectrometry (SIMS); and scanning electron microscopy (SEM).

.I

REPORT DOCUMENTATION PAGE

Form Approved
OMB No. 0704-0188

1a. REPORT SECURITY CLASSIFICATION	1b. RESTRICTIVE MARKINGS
NONE	

2a. SECURITY CLASSIFICATION AUTHORITY	3. DISTRIBUTION/AVAILABILITY OF REPORT
2b. DECLASSIFICATION/DOWNGRADING SCHEDULE	

4. PERFORMING ORGANIZATION REPORT NUMBER(S)	5. MONITORING ORGANIZATION REPORT NUMBER(S)

6a. NAME OF PERFORMING ORGANIZATION	6b. OFFICE SYMBOL (If applicable)	7a. NAME OF MONITORING ORGANIZATION
Howard W. Pickering		Office of Naval Research

6c. ADDRESS (City, State, and ZIP Code)	7b. ADDRESS (City, State, and ZIP Code)
The Pennsylvania State University University Park, PA 16802	Arlington, VA 22217

8a. NAME OF FUNDING/SPONSORING ORGANIZATION	8b. OFFICE SYMBOL (If applicable)	9. PROCUREMENT INSTRUMENT IDENTIFICATION NUMBER

8c. ADDRESS (City, State, and ZIP Code)	10. SOURCE OF FUNDING NUMBERS			
	PROGRAM ELEMENT NO.	PROJECT NO.	TASK NO.	WORK UNIT ACCESSION NO.
	84-K-0201	4315098		

11. TITLE (Include Security Classification)   A Review of the
Mechanism and Kinetics of Electrochemical Hydrogen Entry and Degradation of
Metallic Systems

12. PERSONAL AUTHOR(S)
Pickering, Howard W.

13a. TYPE OF REPORT	13b. TIME COVERED	14. DATE OF REPORT (Year, Month, Day)	15. PAGE COUNT
Annual	FROM 12/15/88 TO 12/14/89	1990 January	54

16. SUPPLEMENTARY NOTATION

17.	COSATI CODES		18. SUBJECT TERMS (Continue on reverse if necessary and identify by block number)
FIELD	GROUP	SUB-GROUP	Review of hydrogen charging and embrittlement; model for determining mechanisms of h.e.r. and H entry and parameters, e.g., H adsorption rate constant; experimental procedures.

19. ABSTRACT (Continue on reverse if necessary and identify by block number)   (Hydrogen Sulfide)

A review of the mechanism and kinetics of electrochemical hydrogen entry and degradation of metallic systems is presented. The partitioning of the discharged hydrogen into molecular hydrogen evolving on the metallic surface and atomic hydrogen entering into a metallic material is considered. A rigorous model has been developed that yields the surface hydrogen coverage, the surface coverage-dependent transfer coefficient of the hydrogen evolution reaction (h.e.r.), and other parameters under a variety of experimental conditions from the permeation data. Further, the catalytic behavior which is quantified by the adsorption rate constant, versus the entry behavior which is quantified by the absorption rate constant, are for the first time determinable by applying the model to the permeation data for various membrane thicknesses. Use of these parameters for analyzing the vulnerability of a solid metallic material to hydrogen entry and subsequent embrittlement is discussed. The model can also successfully analyze the effects of poisons, such as H₂S, on hydrogen entry, and the more complex case of hydrogen entry when the metal is covered with a film on its surface. Keywords: Hydrogen Charging Hydrogen Embrittlement. (AW)

20. DISTRIBUTION/AVAILABILITY OF ABSTRACT	21. ABSTRACT SECURITY CLASSIFICATION
☒ UNCLASSIFIED/UNLIMITED ☐ SAME AS RPT. ☐ DTIC USERS	
22a. NAME OF RESPONSIBLE INDIVIDUAL A. J. Sedriks	22b. TELEPHONE (Include Area Code) (202) 696-4401	22c. OFFICE SYMBOL 1131M

DD Form 1473, JUN 86   Previous editions are obsolete.   SECURITY CLASSIFICATION OF THIS PAGE

A REVIEW OF THE
MECHANISM AND KINETICS OF ELECTROCHEMICAL HYDROGEN ENTRY AND DEGRADATION OF METALLIC SYSTEMS

Rajan N. Iyer and Howard W. Pickering
Department of Materials Science and Engineering
The Pennsylvania State University, University Park, PA 16802.

Our purpose here is to critically review recent advances in understanding the kinetics of the ever elusive and omnipresent hydrogen entry into metallic systems by multiple ways and causing numerous degradation problems, catastrophic in many instances. The problem of hydrogen induced damage and failures is interdisciplinary and varied. For example, in the cathodic protection of metals, in hydrogenation cells where metal electrocatalysts such as Ni are used, in hydrogen energy producing plants and in environments where hydrogen sulfide gas is present as in petroleum refining (1), hydrogen absorption into metals causing degradation of their mechanical properties is the main concern; whereas, in closed systems, such as nuclear reactor cooling pipes, acid container systems, fuel cells, etc., the production of H_2 gas and bubble formation is of great concern not only because of impedances and heat generation, but also because of the explosive properties of hydrogen. Very high pressures of H_2 gas produced by acid corrosion reactions can deform or crack any material employed as a container. Thus, the issue of hydrogen reactions on metallic materials is real, and also quite complex dealing with the adsorption, absorption and/or evolution of hydrogen in metal-hydrogen systems. Attempting here to cover all of the different aspects of the hydrogen problem with references of the vast amount of work done in this field is beyond the scope of this paper. Instead, we will be concentrating mostly on the mechanistic aspects of hydrogen entry into unstressed metallic systems.

It is now understood that hydrogen exists as atomic hydrogen in the dissolved state in metallic components and is similar to interstitial solute atoms such as carbon, as far as diffusional and solubility characteristics are concerned (2). Since hydrogen atoms are the smallest of all atoms, they can be separated into elemental particles of protons and electrons by a simple ionization process. The hydrogen atom can lose its electron to the electronic bands of a metallic material, especially the

tranisition metals such as palladium, as evidenced by the observed linear decrease of magnetic susceptibility with increasing hydrogen content (2).

Quite significant work has been done on hydrogen entry into metals exposed to gaseous hydrogen. In gaseous hydrogen charging, the major reactions occurring on metallic surfaces are the dissociation of H_2 molecules, the adsorption of these hydrogen atoms on the metallic surface and their absorption and diffusion into the bulk metallic phase (2-4). The rate controlling step among these reactions depends on the charging pressure, hydrogen diffusivity in the metallic phase and other factors (5). For example, at high H_2 pressures in the presence of H_2S, adsorption is rate controlling (4). Also, it is possible to have a partial dissociation of molecular hydrogen in the gas phase and this presence of atomic hydrogen in the gas phase can affect the kinetics of hydrogen entry (6). The purity of the hydrogen gas is an important factor for hydrogen entry and embrittlement; for instance, small additions of oxygen reduces hydrogen embrittlement (HE) susceptibility at least at low pressures (7, 8). On the other hand, some hydrogen-containing compounds such as gaseous hydrogen sulfide (9) and water (10) increase HE susceptibility, probably by enhancing the adsorption-absorption kinetics and/or affecting the recombination kinetics (3, 10). In gaseous hydrogen charging, the concentration of dissolved hydrogen in the metal obeys Sievert's law, i.e., the dissolved hydrogen concentration is directly proportional to the square-root of the presssure of hydrogen gas (2). Some of the hydrogen atoms cover the metallic surface as adatoms and this coverage can be determined by a detailed analysis of the sorption kinetics (3, 4, 11, 12). The hydrogen diffusivity and solubility are important parameters for gaging HE characteristics of a material and these can be determined by using gas permeation cells (13, 14). It has been concluded that in general, a ferritic stainless steel is more susceptible to HE than an austenitic stainless steel because the former has a higher hydrogen diffusivity and a lower hydrogen solubility than the latter (15, 16). In spite of the above-mentioned interesting aspects of gas-phase charging and since most cases of hydrogen entry and embrittlement are much more severe in wet environments, the focus of this review in what follows is on hydrogen charging of metallic systems in aqueous environments.

Hydrogen atoms can quickly enter into metallic systems from an aqueous phase. In aqueous solutions, the metal-liquid interface is charged owing to the dipolarity of water molecules (17-19) and the charged interface of the two phases forms a double layer that essentially acts as a capacitor (17, 20). It is because of this capacitive double layer that precise external electronic control or simulation of oxidation/reduction reactions on the metallic phase is possible. In short, the solvated hydrogen ions, H_3O^+, in the aqueous phase can be discharged onto a metallic phase when it is immersed in the aqueous phase by applying a cathodic voltage with an auxiliary (counter) electrode using a galvanostatic or potentiostatic circuit. This is a typical situation in cathodically protected metallic systems. Thus, the two most significant differences between aqueous hydrogen charging and gaseous hydrogen charging are that for the former the charging conditions can be precisely varied and very high fugacities of the order of 10^6 atm. (corresponding to pressures of 10^4 atm.) can be achieved in aqueous hydrogen charging (21, 22). But the kinetics of the aqueous electrochemical hydrogen charging process is very involved as will be evident from the discussion below.

The theoretical analysis of the kinetics of the hydrogen processes occurring at and through the aqueous-metallic interface is based on the electrochemical rate equations. Pioneering work on the hydrogen evolution reaction (h.e.r.) kinetics has been done by Tafel (23), Volmer (24), Horiuti (25), Frumkin (26) and others. Essentially, the hydrogen reduction process involves the reduction of the H_3O^+ ions in the double layer at the metallic surface, followed by two parallel processes which are the evolution of gaseous hydrogen that forms from the adsorbed hydrogen atoms on the surface and the entry of other of these adsorbed hydrogen atoms into the metallic phase itself (27-29). These three steps can take place by different combinations of reaction paths (30, 31). The very first step of H_3O^+ reduction is now fairly well understood to take place by a single electron transfer step:

$$H_3O^+ + e^- = H_x + H_2O \qquad (1)$$

where x refers to the state of the reduced hydrogen atom on the metallic phase.

Immediately, several critical questions can be raised: Where exactly is Reaction (1) occurring and is there a site specificity? How does this reaction take place? What is the state of the reduced hydrogen? What are the possible subsequent reactions? How do these reactions affect the integrity or

3

degradation of the metallic electrode? And quite important, will one of the steps control the rate of the overall process or will it be under mixed control? Can we determine the hydrogen solubility in the metal and its diffusivity, subsurface concentrations and fluxes of hydrogen at various stages, hydrogen coverage on the surface (if indeed it stays there), h.e.r. reaction mechanism and rate parameters and constants of the reactions? Is there a problem with the entry of hydrogen into the metallic phase and if so, what is the problem and what are the controlling parameters? Can we quantitatively evaluate these parameters? Why are some metals and alloys more susceptible to hydrogen embrittlement (HE) than others? Finally, can one control or prevent such problems by alloy design, thermomechanical processing and/or modification of fluid chemistry? And is there an interdisciplinary approach to the problem and solution?

These and related questions have engaged many of the well known electrochemists, corrosion scientists, analytical chemists and metallurgists for the past several decades. Very substantial and significant progress has been achieved by modeling the hydrogen reduction process on the basis of the electrochemical rate theory, as well as by applying fracture mechanics concepts. Still, a general mechanistic theory encompassing quantitative factors and evaluation of critical parameters and constants has not yet been achieved. This is not to say that excellent models and theories don't exist. Indeed, there are elegant models, determinations and calculations describing the transient behavior during hydrogen charging with and without trapping (5, 32-40), which help in determining the solubility, diffusivity, nonsaturable/saturable trap parameters (5) and how deformation creates high binding energy traps for hydrogen (41). Recently, a successful model of the steady state h.e.r. and permeation kinetics has been developed (42, 43) that has the quantitative capacity for evaluating the various rate constants, including the absorption rate constant and the adsorption rate constant and the hydrogen coverage on the metallic surface. It also enables the determination of the operating h.e.r. mechanism. Thus, the model greatly increases the quantitative information that can be obtained from permeation data in comparison to that obtainable from the same data using earlier models (28-30).

Let us now look more closely at the questions raised earlier, particularly the mechanics of the hydrogen evolution and entry processes and how electrochemical rate theory has been quantitatively

4

applied for determining the process mechanisms. It is fairly well agreed that Reaction (1) describing

proton discharge occurs at the metal surface in the case of good electrocatalysts (17, 44). Thus, this

reaction involves discharge of the hydrated protons in the double layer (17) and quantum-mechanical

tunneling (of electrons) across the potential wells in the double layer structure (17, 45, 46). However,

this process, which certainly will be a critical one, has not been well characterized since the quantum-

mechanical parameters such as the discrete energy levels are not directly determinable. Application of

the newly developing powerful technique of scanning tunneling microscopy may prove to be an

invaluable tool to analyze these aspects.

Status of the Reduced Proton and Selvedge Reaction

The question as to the state of the reduced hydrogen was widely debated a few decades ago. It

is now considered that hydrogen attains an adsorbed state on the metallic surface, immediately

following the discharge step (18, 47). But controversy exists as to whether two different forms of

adsorbed hydrogen, such as hydrogen atoms *on* and interstitially *in* the surface are involved as has

been discussed by various workers (18, 48-50). Hydrogen adsorption can cause rearrangement of

surface metal atoms, such as on a nickel surface, as has been shown by low-energy electron diffraction

(LEED) studies (51). Surface adsorption of hydrogen may also lower the fracture stress and cause HE

(52). How exactly hydrogen attains an adsorbed state is even less clear. Much of the work in this area

strongly suggests an intermediate step in which the discharged hydrogen dissolves just under the

metallic surface and equilibrates with hydrogen covering the surface itself (47, 51, 53). This is termed

the absorption-adsorption reaction, which is assumed to be in equilibrium. Although not proven, a

few experimental results (51, 53-57) are consistent with the existence of the absorption-adsorption

reaction, and it may be that the equilibrium condition holds in thicker or low hydrogen diffusivity

metals/alloys. The latter causes the permeation process, itself, to be the slow step in the overall

process, in which case the absorption-adsorption reaction will be in local equilibrium. But for very

thin membranes or for high values of hydrogen diffusivity, the overall permeation process becomes

interface controlled (43, 58). There may be also cases where the intermediate reaction occurs by a more complicated selvedge reaction (42, 43).

The selvedge reaction has been proposed to be the immediate step following the hydrogen discharge step. Its operation would produce a hydrogen concentration profile that is different from that in the rest of the sample (43). The selvedge itself has been defined as an intermediate reaction layer, more than an atomic layer thick, having continuity with the bulk material. The selvedge could be preexisting or be induced by the proton discharge process particularly at high hydrogen overvoltages. Hydrogen transport in the selvedge may occur by a diffusion process in the usual way (in the case of a preexisting selvedge) or by a diffusionless, penetration process that is a part or culmination of the proton discharge step. An example of a preexisting selvedge is a metal with significant surface segregation of minor elements or impurities showing a higher or lower hydrogen diffusivity in the segregated region and a hydrogen concentration profile of smaller or larger slope, respectively, than the slope in the rest of the sample (43). If there are cases where the selvedge reaction occurs by a diffusionless penetration process, the maximum in hydrogen concentration would not be at the cathode surface but at some distance beneath the surface where the penetrating hydrogen protons or atoms come to rest, similar to the situation in ion implanted materials (43). Experimental verification of a selvedge reaction of either type has not yet been carried out. To test the concept of the selvedge reaction, at least one of the available techniques such as neutron scattering (59-61), nuclear magnetic resonance (62) and/or the tritium tracer method (63, 64) may be useful for tracking the motion of the reduced proton.

Detection of a selvedge reaction may prove to be important in explaining some of the less understood physical processes occurring during initial contact of hydrogen with the metal. For instance, intense interaction of hydrogen with the metal may lead to the generation of dislocations which in turn can cause damage such as cracking at or near the metallic surface. In this respect, the selvedge concept is consistent with the observation of dislocation generation in Ti-30 Mo plates during cathodic charging of hydrogen without any applied stress (65). The observation of lattice expansion or contraction in Ti-30 Mo plates sputtered with iron, tantalum or titanium (66) will also be consistent with the selvedge reaction, since the lattice expansion or contraction is due to fine-scale plastic

6

deformation caused by hydrogen charging (without any applied stress). In addition, the selvedge concept will also be consistent with the experimental observation of cracking during hydrogen charging (under no applied stress) (17, 67, 68). Such cracking has been previously rationalized as being caused by extremely high hydrogen fugacities at these locations (67, 68). But the attainment of such fugacities in a very short time in a subsurface region could be facilitated by a diffusionless selvedge reaction which is fast compared with the diffusion of hydrogen, resulting in the highest concentration of hydrogen being located at the selvedge-bulk metal interface rather than at the metal surface. These explanations relating to the selvedge reaction are, however, only tentative at present.

Hydrogen Evolution Reaction (h.e.r.)

It is easy to observe the occurrence of the hydrogen evolution reaction (h.e.r.) since hydrogen gas bubbles are visible through most aqueous solutions. The h.e.r. can occur by more than one route. Proton reduction is the first step and it is followed by either chemical recombination involving the combination of two adsorbed hydrogen atoms or electrochemical recombination involving discharge of a proton directly onto an adsorbed hydrogen atom (17, 29, 47). These are the two well recognized routes of the h.e.r. In general, the h.e.r will occur by both of these routes. There is no evidence the h.e.r. would deletriously or beneficially affect the metallic surface, but it is known to have indirect effects. For example, an enhanced h.e.r. is known to enhance open-circuit corrosion, especially in galvanic couples (69). In crevice and pitting corrosion and even in the intergranular corrosion of sensitized stainless steels, hydrogen gas bubbles have been known to play a major role in causing IR drops and active corrosion (70-78). In many instances, the observation of hydrogen gas bubbles emanating out of pits (73-76) or crevices (73, 76-78), in particular when no hydrogen is evolved at the external surface (where the electrode potential is more noble than the h.e.r. potential), provide ample proof of the existence of both large IR drops within the cavity and the activity of these localized cells. In fact, even the breakdown of passivity of metals and alloys may involve the generation of hydrogen gas at the film-metal interface (79). In contrast to these situations, under hydrogen charging conditions the catalysis of the h.e.r is highly desirable because hydrogen entry will be diminished. This is clearly

7

brought out in the permeation results on iron membranes in which the charging surface consisted also of Pt, Pd, Cu or Ni that showed a reduced hydrogen ingress (80-85). These surfaces were prepared by either electrodeposition on the iron surface or ion implantation into the iron surface layer.

In short, one has to be cautious in interpreting the observation of hydrogen gas evolution in view of its different consequences for hydrogen entry and corrosion of a metallic material. On the other hand, modifying the h.e.r. characteristics by alloying, implantation or surface treatment may provide immunity for the metallic materials to hydrogen entry or corrosion.

Hydrogen Absorption into Metallic Materials

In many situations the greatest concern regarding the application of structural materials is the hydrogen absorption (or entry) reaction because hydrogen is well known to damage the load-bearing ability and/or the toughness of many of these materials (86-98). In order to gain a basic understanding of how and why hydrogen degrades metallic properties, one needs to understand the transport process and kinetics of hydrogen entry, apart from the mechanics of stress and strain. The transport, trapping and especially the kinetics of hydrogen entry are discussed below for hydrogen entry from an aqueous solution under reducing conditions. A treatment of the electrochemical reactions and their rates are indispensable for analyzing the hydrogen entry process. In order to study the hydrogen entry process, in isolation, the potential of a metal electrode is polarized cathodically from its equilibrium redox potential by applying either a constant voltage (potentiostatic) or a constant current (galvanostatic) using an inert counter electrode such as platinum. Under these conditions, protons from the aqueous (electrolytic) phase will be reduced (discharged) on the metal cathode upon which the hydrogen adsorption-absorption reaction proceeds. Most of the discharged hydrogen recombines and evolves as hydrogen gas and the rest is absorbed into the metallic matrix. The absorbed hydrogen permeates into the bulk material. Both the polarization of the h.e.r. and the hydrogen permeation characteristics of a metal cathode are easily measured by using an electrochemical permeation procedure.

Devanathan-Stachurski Electrochemical Cell

To measure experimentally the flux of hydrogen permeating a metallic material, there is an elegant electrochemical device called the Devanathan-Stachurski cell, in which protons are reduced at one surface of a foil or membrane specimen, and the fraction of the discharged hydrogen entering the metallic material and permeating to the other surface is oxidized back to the proton. Details of the set-up and circuitry for this procedure is widely available in the literature (34, 80, 99). The anodic side of the membrane specimen, where the permeating hydrogen is completely oxidized, is usually coated with Pd to prevent corrosion of the specimen. The measured oxidation current provides a measure of the hydrogen flux permeating the membrane thickness.

Membrane Design

The importance of choosing an appropriate membrane thickness (L) to carry out this type of experiment needs to be emphasized. The upper limit for L is controlled by the time to attain a steady state condition. If it takes a very long time (e.g., 2-3 days), then the problems of impurity adsorption at the cathode, change in concentration (especially pH) of the catholyte and background corrosion in the anodic cell, would be encountered. It is, therefore, advised that the time to attain steady state should be well within 24 hours. Once an estimate of the hydrogen diffusivity of the metal/alloy in question is available either from an extrapolation of the high temperature diffusivity data, the literature or trial permeation runs, one can obtain an estimated thickness, $L_e = 2\sqrt{D_L^e t}$ where D_L^e is the estimated diffusivity of hydrogen and t = 24 hours. D_L^e will actually be an effective hydrogen diffusivity rather than the lattice hydrogen diffusivity, if obtained from trial permeation runs, and depends on the hydrogen trapping characteristics of the material. The upper limit for L also has to be chosen after a careful consideration for the sensitivity to thickness of the absorption-adsorption reaction rate constant, discussed subsequently. In addition, one needs to be aware of the lower limit for L, especially for obtaining a realistic value of the hydrogen diffusivity from the transient measurements of the permeation flux. If extremely thin specimens are chosen, then the overall

9

permeation process will likely be surface (interface) controlled (43, 58) or in general, mixed (interface and diffusion) controlled. But a more serious problem in using extremely thin membranes is that either they will be impractical to prepare (or use) or more importantly, grain boundary effects will become dominant. In such thin membranes, grain boundaries will not only short circuit hydrogen diffusion but also localize the hydrogen adsorption and absorption processes. This will mean that the hydrogen diffusivity values, evaluated from the transient permeation measurement, and the adsorption and absorption characteristic parameters, evaluated from the steady state permeation measurement, will not be representative of the bulk material. Therefore, the lower limit for L should be at least five to ten times the average grain diameter.

Besides the thickness, the lateral dimension of the membrane also is an important consideration. In order to avoid edge effects causing significant hydrogen leakage laterally, the L/r ratio should be less than 0.2 (where r is the radius of the membrane exposed to the catholyte) for leakage to be less than 5% (80, 100).

The metallurgical condition of the membrane is also an important consideration. Initial experiments are better carried out on well annealed, high purity specimens in which traps for hydrogen are less of a problem and the hydrogen diffusivity will be closer to the true lattice hydrogen diffusivity. Subsequent experiments can be carried out on specimens having controlled additions of impurities and/or cold work so that these effects can be carefully studied.

Apart from the above considerations, the surface state of the membrane is also important. The surface should be flat, well polished and free of films. However, oxide or other corrosion product films are easily formed on many metallic surfaces and these may affect the kinetics of hydrogen entry and hydrogen transport.

Electrolyte Preparation and Purification

In order to obtain reproducible results, special attention has to be paid to preparing not only the membrane but also the electrolytes. High purity reagents and doubly distilled water, prepared by suggested procedures (101), have to be used when preparing the solutions. For the charging solution

10

(catholyte) there is no pH range that is completely free of problems. In order to avoid corrosive attack of the membrane and pH changes, it is recommended to use slightly alkaline buffer solutions such as borate buffer, as the catholyte; neutral and alkaline solutions are likely to cause the formation of passive layers or other reaction-product layers on the surface. A 0.1M NaOH solution normally serves as a good solution in the anodic cell (anolyte).

It is important to keep the impurities in the solutions to the lowest possible level, since many of the impurities can adsorb on the membrane surface and produce erroneous results. So, pre-electrolysis is a must for both the catholyte and the anolyte. The duration (t) of pre-electrolysis depends on the initial impurity level (c_{oi}), the final (required) impurity level (c_{ti}, say 10^{-10} M), impurity diffusivity in the electrolyte (D_i), electrode area (A_e), solution volume (V_s) and diffusion layer thickness (δ); the relationship is given by (17):

$$t = (V_s/A_e) \, (\delta/D_i) \log (c_{oi}/c_{ti}) \tag{1}$$

The pre-electrolysis is typically carried out for about 72 hours using platinum electrodes at a current of 2 mA, prior to the start of a permeation experiment.

Procedure

After the membrane is fitted into the Devanathan-Stachurski set-up, the anolyte is first introduced into the anodic cell and kept at sufficiently oxidizing potential. Background current is allowed to decay to very low values (< 1 μA) before the catholyte is introduced. The catholyte is introduced at the highest cathodic current, if hydrogen charging is done galvanostatically. At the highest cathodic current, film reduction is both maximized and stabilized for subsequent charging at lower currents. Thus, further film reduction process will not occur at lower cathodic currents, as otherwise interpretation of the permeation measurements will be complicated. In addition, hydrogen trapping will also be saturated and stabilized at the highest cathodic current. If hydrogen charging is done potentiostatically, permeation measurements will be done by starting at the highest hydrogen overvoltage and proceeding to lower overvoltages. It should be borne in mind, however, that the highest cathodic current or overvoltage should be below the critical overvoltage at which irreversible

11

damage such as cracks occur in the material (67, 68). At each applied cathodic current (or overvoltage), steady state hydrogen overvoltage (or cathodic current) and both transient and steady state permeation fluxes are monitored.

Transient Permeation Measurements

By monitoring the hydrogen permeation flux (in terms of the oxidation current in the anodic cell) as a function of time, a wealthy knowledge of the transport properties can be obtained. However, one needs to be very cautious about the procedure and interpretation. An important measurable parameter of the transient permeation curve is the time lag since from this measurement the lattice diffusivity (in the absence of trapping) (5, 36) or the effective diffusivity (in the presence of trapping) (5, 33, 35, 39, 40) is obtained. Analogous to hydrogen trapping analysis using gas permeation experimental data (5), an appropriate electrochemical method to check for the presence of traps in the membrane and if they are saturable or nonsaturable, is to plot the time lag versus the charging current density (i_c). If the time lag does not change appreciably with i_c, then one can reasonably assume that traps are absent; if the time lag decreases with increasing i_c, then saturable traps are present; however, if the time lag increases with increasing i_c, then nonsaturable traps within the range of i_c utilized are present.

Based on Fick's laws of diffusion (36, 100), the transient permeation behavior has been analyzed. In the absence of trapping, the measurable time lag (t_L) has been related to the lattice diffusivity (D_L) and the membrane thickness (L) as (35):

$$t_L = (1/6) L^2/D_L \qquad (2)$$

In the presence of significant trapping, by utilizing an appropriate trapping model the relationship between the time lag (t_T) and D_L would be (5, 36, 40):

$$t_T = (1/6) (L^2/D_{eff}) \qquad (3)$$

where,

$$D_{eff} = D_L (1 + c_T')^{-1} \qquad (3a)$$

$c_T' = \partial c_T / \partial c_L$ can be obtained from the trapping model relating the trapped hydrogen concentration (c_T) and the lattice hydrogen concentration (c_L) (5, 40). This type of relationship assumes that the traps are

12

isolated, ie., do not form an extended network, and that the transport between them is by lattice diffusion (5). Various kinds of defects inside a metallic material can act as traps such as dislocations, grain boundaries, voids, interfaces of other phases, e.g., carbides, with the matrix and impurities. (41). The effective hydrogen diffusivity (D_{eff}) will be affected by the nature of the traps present. Examples follow.

(i) With elastic or nonsaturable hydrogen trapping c_T can be written as equal to βc_L^m and then, D_{eff} will be given by (5):

$$D_{eff} = D_L (1 + m\beta c_L^{m-1})^{-1} \qquad (4a)$$

where β is a trapping constant and m describes the order of trapped clusters, e.g., m = 2 for molecular trapping in voids.

(ii) In the presence of saturable traps, such as dislocations and impurities, c_T can be written as equal to $[(N_T/N_L) K c_L]/[1 + (K/N_L) c_L]$ and then, D_{eff} will be given by (40):

$$D_{eff} = D_L \left[1 + \frac{(N_T/N_L) K}{\left(1+(K/N_L)c_L\right)^2} \right]^{-1} \qquad (4b)$$

where N_T is the trap density, N_L is the number of (interstitial) lattice sites per unit volume and K is the equilibrium constant for the trapping reaction (= exp (E_b/RT), E_b being the trap binding energy). The trap binding energy is an important parameter describing the effectiveness of a trap, especially from the view point of HE, but very accurate transient measurements are necessary to obtain E_b (5). High binding energy traps such as precipitate-matrix interfaces usually cause HE, but not when weaker traps such as dislocations are also present (41). However, the binding energy of hydrogen to traps such as dislocations is higher than the bulk activation energy for diffusion in ferritic (bcc) alloys (41). This may be one of the main reasons why these alloys are more susceptible to HE than fcc alloys and metals (austenitic stainless steels, Ni, etc.) where the opposite is true (102), apart from differences in hydrogen diffusivity and solubility, pointed out earlier.

There is a caution to be observed in the experimental measurements of hydrogen permeation. The main requirement for these measurements to be meaningful for obtaining lattice diffusivity of

13

hydrogen is to ascertain that diffusional conditions indeed hold. This may be done by checking whether $\sqrt{\text{(time lag)}}$ is directly proportional to L. If $\sqrt{\text{(time lag)}}$ is not directly proportional to L, then the permeation process is not under solely diffusional control but rather under either mixed (interface + diffusion) or interface control. Another good test for the diffusional condition can be done under steady state conditions which will be described shortly.

The time lag measurements can be performed on either the rise or the decay transient (103). The break-through time, t_b, representing the time taken for the first hydrogen atoms from the charging side to arrive at the anodic side is also related to D_{eff} as $t_b = (0.5/\pi^2) L^2/D_{eff}$ (104, 105). Of course, the transient behaviour is complicated when reversible or irreversible traps are present in the metallic membrane, which often is the case under HE conditions (67, 106). Anomalies observed in the transient permeation behaviour during hydrogen charging have been associated with irreversible damage (such as void formation and cracking) to the metallic membranes (67, 68). Irreversible damage has been seen to occur only at hydrogen overvoltages greater than a certain critical cathodic overvoltage (68). The hypothesis of a selvedge reaction (42, 43) as well as the high hydrogen fugacities attainable at these high overvoltages would be consistent with this observation.

Hydrogen Solubility and Trapping inside a Metallic Material

From thermodynamic considerations, it is obvious that the hydrogen solubility will be increased with increased hydrogen fugacities since the dissolution of hydrogen in metallic systems can be considered to be taking place with constant heat of solution (22, 41). But constant heat of solution conditions may not hold at very high hydrogen fugacities (where pressure deviates substantially from fugacity). So one would observe 'swelling' or in other words voiding and cracking at very high hydrogen fugacities, as discussed above. Besides the dissolution of hydrogen in the interstitial lattice positions, hydrogen may be trapped at a variety of solid-solid or solid-gas interfaces such as grain boundaries, precipitate-matrix interfaces, dislocation tangles, vacancies and voids within the metallic component (2, 41, 107). The binding energy of hydrogen at these defects depends on the nature of the trapping and of the defects themselves. For example, precipitate-matrix interfaces have higher binding

14

enthalpies for hydrogen than grain boundaries or dislocation cores (41). It is, however, quite difficult to characterize the traps responsible for accumulating hydrogen solely from measurements of binding enthalpies because a mixture of traps of varying binding enthalpies are usually involved. In many cases, surface entry kinetics complicates the analysis of trapping (108). Nevertheless, a partial understanding of trapping may be obtained by special electrochemical techniques.

The transient permeation measurements using the Devanathan-Stachurski technique can be analyzed for trapping characteristics (67, 109). Recently, other experimental techniques such as the potentiostatic double pulse method (110-112) have been utilized to evaluate rate constant for hydrogen trapping at irreversible traps (111, 112). This method is applicable for thicker membranes and the procedure is to charge hydrogen into a metal at a constant cathodic potential for a short time (typically 0.5 to 40 sec), then immediately step the potential to a more positive value (typically 5 to 10 mV negative to the open-circuit potential). In the cathodic transient, hydrogen enters the metal (in addition to evolving as hydrogen gas) but because of the short duration of charging, irreversible traps will remain unsaturated (112). During the anodic transient, hydrogen atoms reoxidize on the cathodic surface and it has been assumed that hydrogen is completely released from the reversible traps, while hydrogen remains in the irreversible traps. Knowing the flux of hydrogen ingress during the cathodic transient and the flux of the anodic transient and using a model of the trap kinetics (110, 111), the irreversible trapping rate constant is determined (112). But the major assumptions in this model are that the irreversible traps are unsaturated during transient hydrogen trapping, the reversible traps release all the trapped hydrogen during the anodic transient, corrosion does not occur during the anodic transient and the surface is film-free during both the cathodic and anodic transients. Also, this technique works well only when the entry process is interface controlled and only when ensured that hydrogen bubbles do not cling to the cathode.

In short, interpretation of the measured transient permeation curves becomes very difficult owing to hydrogen trapping, film reduction processes and impurity adsorption on the cathode. Of particular concern is the reduction of preformed passive films, corrosion product films or adsorbed species on the cathode. The film reduction process depends on the hydrogen overvoltage and

15

therefore, at the highest overvoltage most, if not all, of the film on the metallic surface can be reduced. The film reduction kinetics greatly hampers the reproducibility of the transient permeation measurements and may also affect the attainment of steady state. Since the actual transient curve will include information about the film reduction kinetics, hydrogen transport and trapping parameters cannot be correctly evaluated. The values of hydrogen transport and more so of trapping parameters in the hydrogen permeation literature are often nonreproducible and perhaps unrealistic because of the above-mentioned surface effects (40, 108, 112-114). Even if the films are completely reduced or the film reduction kinetics are stabilized, the trapping kinetics may still not be easily interpretable from transient measurements since independent determinations of trap binding enthalpies and density of traps are not possible. It is therefore advised that hydrogen permeation measurements be performed on high purity, well annealed specimens, with polished, unfilmed surfaces. In this way the transport parameters can be evaluated from transient permeation measurements. The determined lattice hydrogen diffusivity then can be compared with values obtained by other nonequilibrium techniques such as radiotracer (64), mechanical relaxation (115), resistivity relaxation (116), magnetic disaccommodation (117), and equilibrium methods such as nuclear magnetic resonance (118), Mossbauer effect (119) and quasi-elastic neutron scattering (120). On the other hand, the trapping parameters are very difficult to be quantified (114), although a good knowledge can be gained by carrying out transient permeation measurements on metals with controlled additions of impurities or cold work.

The complications in transient permeation experiments such as film reduction processes, will not arise or will be insignificant during steady state hydrogen permeation. This is because the steady state will be attained only after stabilization of all reactions, with the hydrogen discharge, evolution and entry being the only prevailing reactions. Thus, the kinetics of the hydrogen discharge, evolution and entry reactions are best analyzed under steady state conditions.

Kinetics of the Hydrogen Discharge, Evolution and Entry Processes

We have seen how hydrogen enters a metallic phase, although a completely rigorous physical and quantitative knowledge is not yet available. Now we have to understand how each of the steps

16

contributes to the overall h.e.r. and permeation process, how these steps interact with one another and which of the steps will control the overall process. These determinations are best done under steady state conditions, in which case the kinetics of the overall h.e.r. and permeation process can be characterized for a wide range of alloy-environment conditions. In order to analyze the kinetics, it is indispensable to have a model relating the rates of the individual reactions to the driving forces and quantifying interrelationships among various reactions by incorporating boundary conditions and flux and mass balance equations.

Many models (28-30) were developed to understand the relationship between the h.e.r. flux and hydrogen permeation flux for various h.e.r. mechanisms but the partitioning of the discharged hydrogen into molecular (evolving) hydrogen and absorbing (entering) hydrogen was not adequately treated in these earlier models. Hydrogen permeation was assumed to be negligible in order to simplify the flux balance and rate equations. Consequently, these models lacked adequate detailed equations for evaluating the various rate constants, surface coverages and other kinetic parameters relating to hydrogen discharge, evolution and permeation. Only the most probable h.e.r. mechanism could be partly understood. Various reaction schemes were advanced, with the permeation process being diffusion controlled and the discharge-evolution process being coupled or one of these steps (discharge or evolution) rate limiting (30). These deductions were based on determinations of (i) the change in cathode potential, E_C, for every decade change in cathodic current density, i_C, i.e., $dE_C/dlogi_C$ (Tafel slope), (ii) the change in E_C for every decade change in steady state permeation current density, i_∞, i.e., $dE_C/dlogi_\infty$, and (iii) the relationship between i_∞ and i_C. For example, a coupled discharge-recombination mechanism of the h.e.r. would be deduced from a Tafel slope of -120 mV decade^{-1}, $dE_C/dlogi_\infty$ of -240 mV decade^{-1} and i_∞ proportional to $\sqrt{i_C}$ (30). However, a complete quantitative understanding of the kinetics was not possible because of the lack of thorough derivations of the rate equations.

The earlier models have even less value in those cases of significant absorption of hydrogen into metallic materials, such as in poisoned electrolytes (29), since the assumption in these models that hydrogen permeation is negligible is invalidated. A more rigorous model referred to as the I-P-Z

17

model has been developed recently (42, 43) which considers the effect of hydrogen entry into a metallic material on the kinetics of the h.e.r. Let us first consider the steps involved in the hydrogen evolution and entry processes.

Steps in the Electrolytic Hydrogen Charging Process

The overall electrolytic hydrogen charging reaction consists of hydrogen discharge (Reaction (1)), followed by the two parallel reactions of hydrogen gas evolution and hydrogen permeation,

$$H_{ads} + H_{ads} = H_2 \qquad (2a)$$

or

$$H_{ads} + H_3O^+ + e^- = H_2 + H_2O \qquad (2b)$$

and

$$H_{ads} = H_{abs} \qquad (3)$$

Also, as shown, hydrogen evolution can occur either by the combination of the adsorbed hydrogen atoms (Reaction (2a)) or by the electrochemical desorption of the adsorbed hydrogen atom with a proton from the solution (Reaction (2b)). For subsequent discussion, only Reaction (2a) referred to as chemical recombination will be considered for hydrogen evolution. The adsorbed hydrogen in some cases is in equilibrium with the absorbed hydrogen. If the rates of chemical recombination for H_2 evolution and lattice transport (D_l/L) for hydrogen permeation are considered, the lattice transport rate is typically orders of magnitude slower than the surface transport rate of H_{ads} atoms to form H_2 molecules at room temperature. So, of these two parallel reactions, the permeation process will be much slower and the recombination reaction will be the dominant one especially at low coverages and low hydrogen overvoltages. The overall rate of the h.e.r. typically will be determined by the discharge reaction and/or the recombination reaction. At low hydrogen overvoltages, the (potential dependent) discharge reaction will be relatively slow compared to the recombination reaction and therefore the discharge reaction will control the rate of the overall process. But, there are situations in which the recombination reaction is relatively slow, e.g., in poisoned electrolytes, and in this case, the recombination reaction will control the rate of the overall h.e.r. process. In general, the h.e.r. will be

under mixed control. For example, the coupled discharge-recombination mechanism is often prevalent for iron in aqueous solutions (28, 30, 43), but other mechanisms are possible too (28, 43, 57).

The hydrogen discharge reaction rate is given by the cathodic current density, i_c. The relationship between i_c and the cathodic overvoltage, η, is given by the Butler-Volmer equation for a well polarized electrode: $i_c = i_o{}' (1-\theta_H) e^{-a\alpha\eta}$. Here, $i_o{}' = i_o/(1-\theta_e)$, i_o = the exchange current density; θ_H = the surface (hydrogen) coverage, which depends on η; θ_e = the equilibrium surface (hydrogen) coverage (at $\eta = 0$); $a = F/RT = 19.4$ V^{-1} at 25 °C; α = the hydrogen discharge transfer coefficient; $\eta = E_c - E_{eq}$; E_c = the electrode potential during hydrogen discharge; and E_{eq} = the equilibrium electrode potential.

The hydrogen recombination reaction rate is given by $i_r = F k_r (\theta_H)^2$. Here, k_r = the chemical recombination reaction rate constant. The hydrogen permeation rate (at steady state) is given by $i_\infty = F (D_l/L) c_s$. Here, L = the membrane thickness and c_s = the charging (sub)surface hydrogen concentration. If the hydrogen absorption-adsorption reaction is assumed to be in local equilibrium, $c_s = k'' \theta_H$, where k'' = the absorption-adsorption constant that is thickness dependent.

The I-P-Z Model

Assumptions in this model that combines hydrogen evolution and hydrogen permeation are the following: (1) The reactions are at steady state and the only reactions occurring on the cathode surface are hydrogen discharge, chemical recombination and hydrogen absorption. (2) The cathode surface is sufficiently polarized so that no oxidation of hydrogen or any other oxidation reaction can occur at this surface. (3) The absorption-adsorption reaction is in local equilibrium. (4) The hydrogen permeation process involves simple diffusion of hydrogen atoms through the bulk metal. (5) The surface coverage by hydrogen is low enough to follow Langmuir conditions, i.e., the free energy of hydrogen adsorption is coverage independent. This is generally true for $\theta_H \lesssim 0.2$ and $\theta_H \gtrsim 0.8$.

One of the major relationships of the I-P-Z model (42, 43) is between the steady state permeation flux(i_∞) and the hydrogen recombination flux(i_r). Another is the relation between the charging flux(i_c), overpotential(η) and permeation flux(i_∞). These two equations are:

$$i_\infty = k'' (F k_r)^{-0.5} \sqrt{i_r} \tag{5}$$

$$i_c e^{a\alpha\eta} = - (b i_o' / k'') i_\infty + i_o' \tag{6}$$

Equation (5) states that i_∞ is proportional to $\sqrt{i_r}$ and applies for $\eta > RT/F$ and for a relatively fast recombination reaction (i.e., the recombination step is not solely rate controlling); i_r is obtained by subtracting the value of i_∞ from i_c (using Assumption (1)). Previous models (28, 30) have stated that i_∞ is proportional to $\sqrt{i_c}$ for a coupled discharge-recombination process. Equation (5) is an important relationship enabling one to determine the fraction of the hydrogen discharged from the aqueous environment (or solution) that goes off as hydrogen gas and the fraction that actually enters the metal. The constants in Equation (5) consist of the rate constant for the hydrogen recombination reaction, k_r, the rate constant for the hydrogen absorption-adsorption reaction, k'', the Faraday constant, $F=96485$ C/equiv. and $b = L/(FD_l)$.

Equation (6) is derived by considering some electrochemical details of the polarization of the cathode (43). The I-P-Z model is the first of its kind to come up with such a useful relationship. Equation (6) is needed because θ_H cannot be determined by a direct experimental method. θ_H can be indirectly estimated by certain experimental techniques such as the galvanostatic pulse technique and FTIR spectroscopy. The galvanostatic pulse technique (121), consisting of a cathodic pulse followed by an anodic pulse, has been utilized for iron in alkaline solutions yielding θ_H values in the range of 0.05 to 0.12 (53) and in acidic solutions yielding θ_H values in the range of 0.01 to 0.1 (122), with overvoltages in the range of -0.3 to -0.4 V in both cases. But there is an intrinsic problem in using a galvanostatic technique in that at constant current θ_H may not be constant as has been assumed. In fact, θ_H is directly related to the cathodic overpotential rather than cathodic current. Also, there may be appreciable corrosion occurring during the anodic pulse. The FTIR spectroscopy technique for iron in an alkaline solution has yielded θ_H values of 0.08 to 0.16 in the overvoltage range of -0.3 to -0.4 V (57). These values of θ_H are higher than those obtained with the galvanostatic pulse technique. It should be noted that in the FTIR technique, the measurements were made at various constant cathodic electrode potentials. Recognizing the difficulties in obtaining θ_H values in situ during a typical hydrogen permeation experiment, the polarized adsorption isotherm relationships, $\theta_H = 1 - (i_c$

20

$e^{a\alpha\eta}$)/i_o' = bi_{∞}/k'' and $\partial\theta_H/\partial i_{\infty}$ = b/k'', (43) were utilized to derive Equation (6). For this, the transfer coefficient, α, has to be determined by a procedure described elsewhere (43). But accurate determination of α is very important since it is in the exponential term. Construction of true α plots at constant θ_H are discussed in detail elsewhere (123).

The various kinetic parameters such as k_r, k'' and i_o' can be evaluated by plotting i_{∞} versus $\sqrt{i_r}$ (Equation (5)) and $i_c\,e^{a\alpha\eta}$ versus i_{∞} (Equation (6)) and performing regression analyses of these equations (if these plots are linear). Subsequently, θ_H (=bi_{∞}/k'') can be plotted as a function of η and by extrapolating this plot to $\eta = 0$, θ_e can be obtained and, thus, i_o (= $i_o'(1-\theta_e)$) evaluated. The i_o values for various metal electrodes are generally available in the literature for comparison with the i_o values determined using the I-P-Z model. The exchange current density is an important electrochemical parameter for characterizing the catalytic behavior of a metal; e.g., i_o for proton discharge on Pt is about 10^{-3} A cm^{-2} and on Fe is about 10^{-6} A cm^{-2} in pH 1 solutions (17, 69).

Determination of i_o, α, and the various rate constants is important for understanding the electrolytic hydrogen discharge and permeation process and for determining the parameters that control the process. For example, the discharge reaction rate constant, k_1^o (= $i_o'/(a_{H^+}\,e^{-a\alpha E^{eq}})$), gives the rate of proton reduction (a_{H^+} = the hydrogen ion activity and E_{eq} = the equilibrium potential for the h.e.r.). It is directly proportional to the proton jump frequency and exponentially related to the activation energy for proton discharge, while α is related to the symmetry factor describing the ease with which a proton can get to the top of the activation energy barrier (17). Therefore, these two quantities relate to different physical entities, k_1^o describing the discharge kinetics and α describing the characteristics of proton transfer across the double layer. The activation energy for hydrogen discharge is thus overcome by the cathodic potential (driving force) across the double layer with the ease of electron and hydrogen transfer (displacement) determined by α and the rate given by the cathodic current. The chemical recombination kinetics are characterized by k_r that describes the surface diffusion of hydrogen, mean displacement for hydrogen recombination and site specificity, if any.

In order to understand the h.e.r. mechanism and rate controlling step, if any, the intrinsic (coverage-independent) rates (i.e., the rate constants) of the discharge ($v_d = k_1^o\,(a_{H^+})\,e^{-a\alpha E^{eq}}$) and

of the recombination ($\upsilon_r = k_r$) reactions have to be compared. If υ_d and υ_r are within one order of magnitude of each other, then the discharge and recombination reactions are considered to be coupled (17, 43). If the reactions are coupled, any factor that changes the rate of one reaction will affect the rate of the other reaction as well as the rate of the overall reaction. For example, if the pH of the electrolyte or the cathodic potential is changed it will directly affect υ_d and in a coupled discharge-recombination process, it will also affect υ_r.

The hydrogen absorption-adsorption rate constant, k'', is a very important parameter characterizing hydrogen absorption and adsorption. It contains quantitative terms describing surface and subsurface kinetic properties of the metal-hydrogen interaction. If k'' is increased, hydrogen absorption is enhanced and if k'' is decreased, hydrogen evolution is enhanced. The k'' values can be altered by the presence of films or adsorbed species on the surface, or impurities in the metal. However, until recently it was not possible to determine k''.

If the absorption-adsorption reaction is in local equilibrium, a complete steady state flux balance at the subsurface will yield (53, 58): $i_\infty = F k_{abs} \theta_H - F k_{ads} c_s$, where k_{abs} is the hydrogen absorption rate constant and k_{ads} is the hydrogen adsorption rate constant, and $(i_\infty)^{-1} = [k_{ads}/(FD_l k_{abs} \theta_H)] L + (F k_{abs} \theta_H)^{-1}$. Under diffusion controlled permeation conditions, i.e., i_∞ is inversely proportional to L, the latter relation becomes (43, 58): $i_\infty \cong F(D_l/L) k' \theta_H$, where $k' = k_{abs}/k_{ads}$. This steady state criterion will thus serve as an additional check for the diffusion controlled condition, apart from the transient stage condition of the square-root of time lag being proportional to L. On the other hand, for very thin membranes the process will be interface contolled. In this case, $i_\infty \cong F k_{abs} \theta_H$ and thus k_{abs} can be evaluated (58). The importance of evaluating k_{abs} for quantitatively understanding hydrogen entry kinetics and embrittlement in metallic materials have been emphasized (53, 58). However, preparing extremely thin membranes or using them in a permeation cell is impractical. Besides, in overly thin membranes grain boundaries may not only localize the absorption-adsorption reaction but also short circuit hydrogen transport through the membrane and, therefore, bulk properties are not adequately evaluated. To overcome this problem, L has to be at least five to ten times the average grain diameter for a polycrystalline membrane.

The I-P-Z model provides an analytical means of evaluating both k_{abs} and k_{ads} using a range of membrane thicknesses that avoid the above-mentioned problems. The relationship is given by (43):

$$(k'')^{-1} = (k_{ads}/k_{abs}) + (D_l/k_{abs})(L)^{-1} \qquad (7)$$

Thus, by determining k'' as a function of L, k_{abs} and k_{ads} are easily found (if the $(k'')^{-1}$ versus $(L)^{-1}$ plot is linear). The L values have to be chosen within a small dimensional window, typically ten to a few tens of the grain diameter since, in addition, if the membrane is too thick, $(k'')^{-1} \cong (k_{ads}/k_{abs})$, and so k'' becomes thickness independent.

The reaction rate constants and the related free energies follow the Arrhenius relationship. Thus, k_{abs} is proportional to $e^{-(\Delta G_{abs}/RT)}$ and k_{ads} is proportional to $e^{-(\Delta G_{ads}/RT)}$, where ΔG_{abs} and ΔG_{ads} are the activation energies of hydrogen absorption and adsorption, respectively, and T is the temperature in K. If the plots of $\log(k_{abs})$ versus $(T)^{-1}$ and $\log(k_{ads})$ versus $(T)^{-1}$ are linear, then ΔG_{abs} and ΔG_{ads} can be determined. What this involves simply is carrying out hydrogen permeation experiments for various membrane thicknesses at different temperatures and all the useful quantities can be determined. At present, there are no proper alternative ways of determining k_{abs} and k_{ads} and therefore, these values are not easily directly verified. However, the activation energies can be determined by using experimental techniques such as pseudocapacitance (47) and B.E.T. (50, 124, 125). Such determinations can also be compared with those obtained in gas phase hydrogen charging, correcting for the fugacities involved. These approaches may offer unique means of not only correlating aqueous charging data to gas phase charging data but also provide a broad unification of the entry and embrittlement by hydrogen originating from two independent hydrogen sources. Making this connection between gas-phase and aqueous-phase charging may be possible because the absorption and adsorption processes relate to specific material-hydrogen interaction characteristics independent of the source of hydrogen.

Modified I-P-Z Model for Poisoned Electrolytes

The basic I-P-Z model assumes Langmuir conditions and as pointed out earlier, this will be certainly valid if θ_H is very low. However, when metallic materials encounter deleterious

23

environments, typical of many real applications such as those containing the so called poisons, the hydrogen permeation is significantly enhanced indicating significant coverages of the surface by hydrogen in which case the Langmuir condition may no longer hold. A poisoned electrolyte commonly encountered by iron and its alloys is hydrogen sulfide in acidic and alkaline solutions.

Hydrogen sulfide in acidic solutions: The problem of enhanced hydrogen entry caused by the presence of poisons such as H_2S in acidic solutions has been analyzed by various investigators (28, 126-132). Although many different mechanisms (28, 126-128, 130) were considered, due to a lack of a quantitative model a rigorous analysis had not been achieved. The mechanisms proposed include dissociation of H_2S to provide another source of hydrogen discharge as well as adsorption of HS⁻ or S⁼, slowing (poisoning) of hydrogen recombination and H_2S functioning as a bridge for hydrogen discharge. But in acids (pH < 5), dissociation of H_2S is unfavorable. If the poisoning mechanism is considered, an increase in the h.e.r. overvoltage has to be observed which is not the case for H_2S in acids (133). So, the bridge mechanism (126) that proposes a decrease in h.e.r. overvoltage, accompanying the increased hydrogen entry, is more likely to be operating. For quantitatively analyzing the mechanism and determining the various kinetic parameters, the I-P-Z model has been applied after modifications taking into account the significant hydrogen coverages. Equations (5) and (6) were modified to include the Frumkin-Temkin correction for the discharge and chemical recombination rate equations (47). Two important equations were then obtained (133):

$$\log_e (\sqrt{i_r}/i_\infty) = (\alpha f b/k'') i_\infty + \ln(b(Fk_r)^{0.5}/k'') \tag{8}$$

$$\log_e (f_{i_c,i_\infty}) = -\alpha a \eta + \ln(i_o') \tag{9}$$

where

$$f_{i_c,i_\infty} = i_c \, e^{(\alpha f b i_\infty/k'')}/(1-b i_\infty/k'') \tag{9a}$$

Here $f = \gamma/RT$, where γ is the gradient of the apparent free energy of adsorption with coverage and the value of $f = 4.5$ has been assumed. However, an accurate value of f has to be obtained for each specific metal-solution system for a more rigorous analysis; techniques such as the adsorption pseudocapacitance measurements (47) can be utilized for evaluating f. Once f is known, Equations (8) and (9) will unambiguously yield the values of α, k'', k_r and i_o'. A detailed evaluation procedure is

24

described elsewhere (133). Essentially, log $(\sqrt{i_r}/i_\infty)$ versus i_∞ is plotted and if this plot is linear, the slope and intercept will contain the values of α, k'' and k_r. Then, in Equation (9), k'' can be expressed in terms of α and iteratively solved for α. If α values converge to a fixed value, it will indicate that $\log(f_{i_c}, i_\infty)$ is linear with η. But if α does not converge, it will indicate that the system is not following these relationships and that one or more of the assumptions may not be valid. Such cases can arise if the recombination reaction becomes rate limiting or if it involves electrochemical desorption (Reaction (2b)). If α does converge, then k'', k_r and $i_o{}'$ are easily evaluated by regression analyses of Equations (8) and (9). These quantities provide very useful information about the way in which poisons promote hydrogen entry. For example, it has been found that a large hydrogen entry into the metal occurs when H_2S is present in highly acidic solutions, but the hydrogen overvoltage is reduced. Analysis with the modified I-P-Z model showed that the increased hydrogen entry is largely due to the recombination step being slowed considerably probably in conjunction with the reaction:

$$H_2S + e^-_{cathode} \rightleftharpoons H_2S^-_{cathode} \tag{4}$$

This side reaction can occur quite fast at the cathodic metal surface and affect the discharge and recombination steps in various ways (133):

(1) H_2S can work as a bridge for hydrogen discharge through H_2S^-, as originally proposed by Kawashima *et al* (126):

$$H_2S^-_{cathode} + H_3O^+ + M \rightarrow M\text{-}H + H_2S + H_2O \tag{5}$$
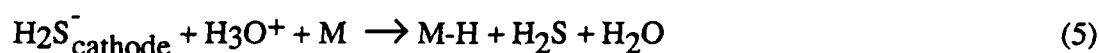
Reaction (5) leads to a decrease in the overvoltage for the discharge reaction.

(2) The recombination reaction can be poisoned by the $(H...H_2S)$ intermediate forming on the cathode and slowing the diffusion of H adatoms and/or blocking the recombination sites (if the recombination reaction is heterogeneous) on the metallic surface.

If the chemical recombination reaction is highly poisoned such as by a high $[H_2S]/[H^+]$ ratio, then the evolution reaction can occur by the alternate electrochemical desorption route (Reaction (2b)). Thus, electrochemical desorption becomes more probable at higher pH for a specific H_2S

concentration in the solution. Such an occurrence has been reported for iron (99.9% pure) in acetate solutions of pH > 3 in the presence of H_2S (134).

The value of α obtained using I-P-Z the model, slightly increased with small additions of H_2S, consistent with the Kawashima *et al* bridge mechanism. Thus, the primary function of H_2S^- acting as a bridge is to facilitate transfer of protons across the double layer and, thus, decrease the overvoltage necessary for hydrogen discharge. But the intermediate product (H...H_2S) poisons the recombination reaction and this has been quantitatively illustrated by the precipitous decrease in k_r with small additions of H_2S. This is further quantified by the increase in θ_H with increasing [H_2S] at a particular η showing the build up of H adatoms due to slowing down of the recombination reaction.

The model evaluations also showed that k'' increased with increasing [H_2S], although not significan... This (small) effect may be a result of change in adsorption energy with coverage, since any change in adsorption energy will also alter k_{ads}. In addition, one cannot rule out adsorption of HS^- due to a partial dissociation of H_2S into HS^- and H^+ even in highly acidic solutions. This is because the pH at the metal-solution interface can be kinetically shifted to higher pH as a result of the proton reduction process. Thus, in order to attain a complete picture of the role of H_2S in enhancing hydrogen entry into metallic materials, the adsorbates have to be experimentally analyzed.

Hydrogen sulfide in alkaline solutions: The synergistic effect of pH and H_2S leads one to deduce that electrochemical desorption will be significant in alkaline solutions. In solutions with very high pH values, H_2S will dissociate into HS^- or even into $S^=$. The result will be that the mechanism of enhancement of hydrogen entry by H_2S will be different in alkaline solutions. Indeed, this has been found to be the case in pH 10 solutions (135). A more general model is needed for considering both the chemical recombination and electrochemical desorption routes for hydrogen evolution with significant hydrogen coverages; the equations take the form (135):

$$\log_e (U/Z) = \alpha (a\,\eta + 0.5\,f\,Z) + \log_e (0.5\,F\,k_r) \tag{10}$$

$$Y = -[4\,k_{ed}/(F\,i_o')]\,X + 4/(F\,i_o') \tag{11}$$

where

$$U = \sqrt{\{(F\,k_{ed})^2 + F\,k_r\,(i_{ct} - i_\infty)\,e^{2a\alpha\eta}\}} - F\,k_{ed}$$

$$W = \{4\,U\,e^{-2a\alpha\eta}/(F\,i_o{}'\,k_r)\}\,\{i_{ct}\,e^{2a\alpha\eta} - (k_{ed}/k_r)\,U\}$$

$$X = U\,e^{-2a\alpha\eta}/(k_r\,i_{ct})$$

$$Y = k_r\,W/(U\,i_{ct})$$

$$Z = 1 - \sqrt{1-W}$$

Although Equations (10) and (11) are quite complex, all the unknown quantities such as α, the chemical recombination (Tafel reaction) rate constant, k_r, the electrochemical desorption (Heyrovsky reaction) rate constant, k_{ed}, and $i_o{}'$ can be evaluated by iterative regression analysis of these equations. It is to be noted that the cathodic current density, i_{ct}, is a sum of the discharge current density, i_c, and electrochemical desorption current density, i_{ed}. At steady state, $i_c = i_r + i_{ed} + i_\infty$, where i_r is the chemical recombination current density. If the values of α, k_r, k_{ed} and $i_o{}'$ converge to fixed values, then $\log(U/Z)$ versus $(a\,\eta + 0.5\,f\,Z)$ and Y versus X plots will be linear, indicating applicability of these relationships to the particular metal-solution system.

By applying this model to the experimentally measured variables of i_{ct}, η and i_∞ for Ferrovac iron in pH 10 solution with varying concentrations of H_2S, it has been found that k'' is increased significantly due to H_2S. Other parameters such as α, $i_o{}'$ and the variable θ_H are not affected significantly by H_2S. The increase in k'' means that k_{ads} is decreased with respect to k_{abs} and this is possible by the adsorption of HS^- or even formation of a sulfide film by reaction of $S^=$ with the surface. Hydrogen permeation measurements carried out on pyrite (FeS) showed that both hydrogen solubility and diffusivity are about an order of magnitude higher than on Fe (136). This has an implication on how a sulfide film may promote entry of hydrogen into iron from aqueous solutions. In the section on a composite I-P-Z model for the analysis of filmed metallic surfaces, this aspect will be examined. It is quite possible that H_2S enhances hydrogen permeation in iron and its alloys by breaking down or modifying passive films and/or suppressing the recombination reaction (129).

pH Effect in the Hydrogen Process

The synergistic effects of pH and H_2S concentration, $[H_2S]$, have been studied in the previous section. Let us now look more closely at the effect of pH by itself. When the pH is lower, $[H^+]$ increases and the rate of hydrogen discharge will increase since i_o increases with increasing $[H^+]$. But as hydrogen discharge occurs at the cathode, the pH close to the double layer is expected to increase especially in unbuffered solutions. In solutions where the ionic mobility is low such as when metal complex ions form, this effect may become quite significant. But if the pH is close to the equilibrium pH of the hydrolysis reaction for the solution, or if the solution is buffered, the pH will cease to be a significant variable. In less acidic, neutral or alkaline solutions, the presence and role of corrosion products on metallic surfaces will become quite important for both the h.e.r. and hydrogen entry. Even at fairly significant cathodic overvoltages the corrosion-product films can be quite stable for many base metals. Although some investigations have been carried out on hydrogen permeation through protective films (137-140), the process is still poorly understood. The complications stem mainly from the unknown electronic, chemical and physical (particularly diffusion and ion migration) properties of the protective films. Significant hydrogen trapping should be quite prevalent in the protective film as a result of the expected bonding between $O^=$ (and/or OH^-) and protons (H^+). Also, a significant potential (IR) difference is expected between the metal-film and film-solution interfaces owing to the generally poor electronic conductivity of the film. Some models of hydrogen trapping have considered pure diffusion of hydrogen through the film (137), yet some others invoke transport of hydrogen by activated jump of the protons induced by the potential difference across the film (140). The major problem in sorting out the role of protective films on the hydrogen process is that it is difficult, if not impossible, to attain a completely film-free surface and perform hydrogen charging on a pure metallic surface, especially for metals and alloys of interest such as Fe, Ni and Al. In chloride solutions, it may be easier to a obtain film-free surface but due to specific adsorption of Cl^- in the inner Helmoltz layer (IHL) (141) of the double layer, the characteristics of the hydrogen process will be altered and another unknown variable will be introduced.

Composite I-P-Z Model for Filmed Metallic Surfaces

In many actual situations a metallic surface is covered with corrosion products, such as oxide or hydroxide films that may be protective or passive and in many cases act as barriers for hydrogen entry. The hydrogen discharge and the absorption-adsorption reactions will be occurring in the film phase. Also, hydrogen will diffuse through the film, enter the metal and diffuse through the bulk of the metal. Therefore, the mechanism and kinetics of hydrogen evolution, entry and permeation can be greatly modified as a result of the film. A composite I-P-Z model considering the role of the film in the hydrogen process has been recently developed (142). This model has a few assumptions. One of the main assumptions is that the hydrogen absorption-adsorption reaction (ie., the equilibrium intermediate reaction) occurs exclusively in the film phase. This is reasonable if the absorption-adsorption reaction occurs at the film-solution interface. However, if the selvedge reaction (ie., the non-equilibrium intermediate reaction) occurs, then it will be necessary to critically check this assumption. The model also assumes that chemical reaction or trapping of hydrogen in the film or the metal does not occur during steady state. Another major assumption in the model is that hydrogen diffuses as atoms through the film and the metal. In other words, proton migration is not considered. There are a few reports in the literature (139, 140) citing the diffusion-activated jump or the migration of protons in the film. But it is almost impossible at this time to model this complex situation since the diffusivity of H^+ and the field across the film are functions of several unknown variables, e.g., position, time, ratio of OH^- to $O^=$, and so their characterization is a formidable task. By virtue of these considerations, the assumption of an effective diffusivity of hydrogen in the film is acceptable in view of the present state of knowledge of hydrogen transport in the film. In the simpler special case of the model, it is assumed that there is a negligibly small abrupt change in concentration at the film-metal interface, whereas if the hydrogen solubilities are largely different in the film versus the metal, a large gradient in hydrogen concentration can be expected across the film-metal interface. The model further assumes that there is no accumulation of hydrogen at the film-metal interface during steady state, i.e. if the film-metal interface has defects such as dislocations and voids, then hydrogen can accummulate there but once steady state is achieved no futher accummulation will occur. The problem of the hydrogen accumulation at the film-metal interface could be important from the view point of HE.

Nothwithstanding these many assumptions, the following model provides a starting analytical procedure for investigating the role of a film on hydrogen entry. Analysis of the flux balance at the film-metal interface yields (142): $(i_\infty)_f = (i_\infty)_m$ and then, since $(i_\infty)_f = F\, c_{s,f}/[L/D_l + L_f/D_f]$ and $(i_\infty)_m = F\, [k_{abs,f}\, (c_{s,f}/k'') - k_{ads,f}\; c_{s,f}]$,

$$(k'')^{-1} = (k_{ads,f}/k_{abs,f}) + (D_l/k_{abs,f})\,(L+\lambda)^{-1} \tag{12}$$

Here, $(i_\infty)_f$ = steady-state hydrogen permeation flux through the film; $(i_\infty)_m$ = steady-state hydrogen permeation flux through the metal; $c_{s,f}$ = hydrogen concentration just beneath the surface (subsurface) of the film; L_f = film thickness; D_f = hydrogen diffusivity in the film; $k_{ads,f}$ = hydrogen adsorption rate constant for the film; $k_{abs,f}$ = hydrogen absorption rate constant for the film; and λ = effective film thickness = $L_f\,(D_l/D_f)$.

Equation (12) shows that the film can affect not only hydrogen adsorption and absorption but also hydrogen transport depending on the relative magnitudes of λ and L. Since the value of λ is not usually known, it has to be eliminated by twice differentiating Equation (12) with respect to L, yielding (142):

$$(k'')^{-1} = 2\, f_{k''}\,(L) + (k_{ads,f}/k_{abs,f}) \tag{13}$$

where

$$f_{k''}\,(L) = [\partial(k'')^{-1}/\partial L]^2/[\partial^2(k'')^{-1}/\partial L^2] \tag{13a}$$

since λ does not depend on L. The k'' value can be determined as a function of L as described in the Basic I-P-Z model section.

Thus, if the plot of $(k'')^{-1}$ versus $f_{k''}\,(L)$ is linear with a slope of 2, then Equation (13) is applicable for analyzing hydrogen permeation through filmed metals and the intercept of this plot will give the value of $(k_{ads,f}/k_{abs,f})$. Rearranging Equation (12), one can obtain the following relationship:

$$[(k'')^{-1} - (k_{ads,f}/k_{abs,f})]^{-1} = (k_{abs,f}/D_l)\,L + (k_{abs,f}/D_l)\,\lambda \tag{14}$$

So, if the plot of $[(k'')^{-1} - (k_{ads,f}/k_{abs,f})]^{-1}$ versus L is linear and D_l is known, then $k_{abs,f}$ and λ can be evaluated from the slope and the intercept, respectively and then, the value of $k_{ads,f}$ can also be evaluated. If the film is very thin, λ will be very small and cannot be resolved from the error in the

30

above evaluations. However, the values of $k_{abs,f}$ and $k_{ads,f}$ will indicate whether the metallic surface

is filmed or not, if these values are already known for the unfilmed surface. This is often not

otherwise known. Therefore, an alternative analytical procedure has been developed (142). This film

analysis is fairly simple, using the set of values of k'' as a function of L and differentials of $(k'')^{-1}$ with

respect to L. The following relationship is derived from Equations (12) and (13):

$$L [g_{k''} (L)] = [1 + (\lambda/L)]^{-1} \tag{15}$$

where

$$g_{k''} (L) = -2 [\partial (k'')^{-1}/\partial L]/[\partial^2 (k'')^{-1}/\partial L^2] \tag{15a}$$

Also, from Equation (12), one obtains the following:

$$L (k'')^{-1} = (k_{ads,i}/k_{abs,i}) L + (D_l/k_{abs,i}) [1+(\lambda/L)]^{-1} \tag{16}$$

where the subscript i represents f (for film) or m (for metal).

Equations (15) and (16) can be utilized for the film analysis. Plots of L $[g_{k''} (L)]$ versus L or

L^{-1} and $L(k'')^{-1}$ versus L are shown in Figures 1 and 2. If the metal is unfilmed, or if the film does

not affect the kinetics of hydrogen entry, then $\lambda \sim 0$, $k_{ads,i} = k_{ads,m}$, $k_{abs,i} = k_{abs,m}$ and $L[g_{k''}$

(L)] will be independent of L (Figure 1A). If additionally, $L(k'')^{-1}$ is proportional to L (Figure 2A),

then hydrogen entry is controlled by the bulk diffusion of hydrogen through the metallic membrane.

But, if $L(k'')^{-1}$ is independent of L (Figure 2B), then the hydrogen entry is controlled by the metal-

solution interface. On the other hand, if the hydrogen entry is under mixed control, then $L(k'')^{-1}$ will

be linear with respect to L, with a positive intercept (Figure 2C).

The second case (Figure 1B) will arise if L $[g_{k''} (L)]$ decreases linearly with respect to L^{-1},

with an intercept of 1. This will indicate that a film such as a passive film, is present ($\lambda > 0$), but that

$\lambda << L$ so that L $[g_{k''} (L)] \cong 1 - \lambda L^{-1}$. This may be observed in many real systems, since usually

$(L_f/L) << 1$ (typically $L_f \sim 5$ nm and $L \sim 0.1$ mm) and $(D_f/D_l) << 1$ (typically less than 10^{-2}). In

order to know whether this film is affecting hydrogen entry kinetics or not, one also looks at the plot

of $L(k'')^{-1}$ versus L to determine whether the hydrogen entry is metallic bulk diffusion controlled

(Figure 2A), interface controlled (Figure 2B) or under mixed control (Figure 2C). However, in the

case of interface control, if it is indeed film-solution interface control, then $k_{ads,i} = k_{ads,f}$, $k_{abs,i} =$

$k_{abs,f}$. If this is found, one can deduce that the film, such as a passive film, is greatly influencing absorption and permeation of hydrogen. So, any agent that modifies or breaks the film will change the hydrogen entry characteristics and can directly affect hydrogen embrittlement susceptibility. This is illustrated in the case of H_2S depassivating the iron surface, poisoning the h.e.r. and, thus, enhancing hydrogen entry into iron (129). Another illustration is in the case of mechanical strain rupturing a passive film and increasing hydrogen absorption resulting in hydrogen assisted failure in a 4340 steel under cathodic polarization in aqueous sodium chloride solution (143). Thus, the film can influence the hydrogen entry and evolution processes and a quantitative understanding can be gained by the film analysis using the I-P-Z model.

In a few special cases, it may happen that $\lambda \sim 0$, although a film is present. This can occur if $(D_f/D_l) > 1$ such as in the case of a sulfide film on iron (136). In this situation, the film is not limiting hydrogen transport. But it may change k_{ads} and/or k_{abs} and also the subsurface hydrogen concentration, c_s, since hydrogen solubility is higher for the iron sulfide compared to that of iron (136) and can thus enhance hydrogen permeation into iron.

A third case of the composite I-P-Z model arises when λ and L values are comparable (Figure 1C). This may be the case if the film is too thick such as a thick oxide covering a metal, or if the membrane is too thin. Here, at L $[g_k'' (L)] = 0.5$, $\lambda = L$ (Figure 1C) and the film will solely control the h.e.r. and the hydrogen permeation process will be under mixed control. The transport of hydrogen may involve migration of protons, in addition to diffusion of hydrogen atoms, since the potential drop in the film will be substantial. But due to a lack of knowledge of the potential field distribution in the film and migration properties of protons in the film, a simple diffusion process of hydrogen has only been considered in this model. To determine whether the film is acting as a barrier or instead, affecting the hydrogen adsorption-absorption process, film thickness, L_f, can be varied indirectly by varying the starting highest cathodic overpotential, η_{hi}, at which a particular permeation experiment is carried out. L_f is expected to decrease with increasing $|\eta_{hi}|$. This electrochemical procedure will be useful in distinguishing between film transport control of the overall rate and the absorption-adsorption reaction at the film surface controlling the overall rate. Since λ is proportional

32

to L_f and since L_f is an inverse function of $|\eta_{hi}|$, increasing $|\eta_{hi}|$ means decreasing λ. From Equation (15) it is easily seen that as λ is decreased, $L [g_{k''} (L)]$ is increased. So, if hydrogen diffusion through the film is rate controlling, $L [g_{k''} (L)]$ will increase monotonically with increasing $|\eta_{hi}|$ (Figure 2D). But, if hydrogen entry is film-solution interface controlling, $L [g_{k''} (L)]$ will not change with $|\eta_{hi}|$ (Figure 2E).

Hydrogen Embrittlement of Metallic Materials

Until now, the kinetics of hydrogen absorption and the entry charactertistics in metallic materials have been critically examined. Hydrogen solubility, diffusivity and trapping characteristics have also been briefly discussed. The absorbed and trapped hydrogen can synergistically interact with an applied or residual stress to cause embrittlement failure in many metallic systems, especially in those with high yield and tensile strengths (144). How exactly hydrogen causes embrittlement in many metal/alloy-environment system is not understood in a basic and quantitative sense. We have seen how hydrogen enters into a metallic material from the aqueous environment in a fairly basic quantitative manner. This is possible because hydrogen fluxes and potentials are measurable by a simple electrochemical permeation technique. The measurements can be quantitatively interpreted with the recently developed I-P-Z model and pertinent kinetic parameters can be evaluated. However, the interaction of hydrogen (that is absorbed in the lattice or more significantly trapped at defects) with stress fields in the material is immensely complex to analyze by a physical and mathematical model. Current understanding of the hydrogen embrittlement mechanism is essentially phenomenological, for specific metal/alloy-environment systems. Due to this, a unified mechanistic theory has not emerged, but instead a string of phenomenological mechanisms have been proposed.

In a broad sense, two classes of metallic materials susceptible to HE can be identified - hydride formers such as Al, Ti, Zr and Nb, and non-hydride formers such as Fe, Ni and Cu. In hydride formers, the HE mechanism is fairly well understood. In metallic systems such as Nb (145), Al (146) and Zr (147), stress induced hydride formation results in significant elastic and plastic accommodation strains around the precipitated hydride due to a decrease in dislocation mobility and slip systems,

33

especially at high stresses, and fracture ensues. The hydride precipitates thus act as embrittling sites for cracking under stress. Propagation of cracks usually involves repeated formation and breakage of the brittle hydride precipitates (93, 148). In non-hydride formers, however, the HE mechanism is not well understood. The following phenomenological mechanisms have been proposed:

Pressure mechanism: Hydrogen atoms trapped at a void or at an interface between an inclusion and lattice can precipitate as molecular hydrogen and build up pressure, adding to the applied stress (107, 144, 149). This mechanism is relevant for understanding blistering and dimple rupture, especially in low strength steels (107). But the pressure mechanism cannot explain brittle behavior in high strength steels due to hydrogen charging (107, 144), especially at low pressure hydrogen gas (7).

Surface energy reduction mechanism: In this case, the adsorbed hydrogen (rather than the absorbed hydrogen) plays the role in the cracking process. This mechanism is similar to Griffith's crack model (107, 148) in that the surface energy of the crack surfaces is lowered by adsorbed hydrogen, especially that on clean metallic surfaces (150). The lowering of fracture energy by adsorbed hydrogen promotes cracking. Although this mechanism may be operating in a few cases, it cannot explain the commonly observed HE characteristics such as discontinuous crack propagation and reversal of brittle delayed failure on stress removal (41). Also, this mechanism cannot explain why other species such as oxygen, that adsorb more strongly than hydrogen do not embrittle metals (107).

Decohesion mechanism: Here, the reduction in fracture energy is proposed to occur not at the surface but within the bulk of the metal such as at grain boundaries or other interfaces whose interatomic cohesive force is lowered by hydrogen (151-153). This will account for the specificity of hydrogen for embrittlement since hydrogen can be easily transported deep into the material even at room temperature. Hydrogen can break the bonds at the crack tip resulting in HE, especially in high strength steels (22, 151, 154). In this mechanism, hydrogen accumulates at the root of a notch or crack front and the crack propagates in a discontinuous manner, which has been shown by resistivity measurements (154). Perhaps, this mechanism is by far the best in explaining many observations of HE cracking process. However, without a better understanding of the electronic interaction between

34

protonic hydrogen in solid solution and the bonding forces of the metallic lattice, the exact mechanism by which hydrogen can reduce cohesive strength will not be known (144).

Dislocation mobility mechanism: This mechanism proposes that hydrogen may be promoting dislocation motion and cause either localized softening behavior (155) or hardening behavior (156, 157). Various schemes have been suggested to rationalize this concept. For example, moving dislocations can drag hydrogen into microvoids and deposit hydrogen in large concentrations when the hydrogen carrying dislocations are annihilated by microvoids (156, 158, 159). But the kinetic supersaturation of hydrogen due to such a process has been shown to be small and insufficient to explain HE (160). In iron alloys and nickel, softening behavior has been observed under specific conditions of hydrogen presence (161-163). The softening effect due to hydrogen has been considered to arise from (162) (a) a decrease of the Peierls stress due to the presence of solute hydrogen or carbon, or (b) a decrease in the energy required for double kink nucleation on screw dislocations due to hydrogen, or (c) a decrease in the effectiveness of other solute pinning species due to the presence of solute hydrogen. Enhancement of screw dislocation velocity and multiplication of dislocations due to hydrogen have been observed in nickel and iron (161, 164). These aspects explain initial softening behavior; subsequently, hardening can occur due to dislocation interactions (161, 165). Such processes can cause localized deformation at slip planes close to the crack tip with consequent local thinning near the crack (166). The result is that plastic instability leading to hydrogen embrittlement along the active slip planes and transgranular crack propagation along the slip planes become possible (161, 166). Although these concepts explain some aspects of the fracture process, it is not still established whether hydrogen atoms can act as effective solute for dislocation interaction like massive elements such as C. Also, it has not been established whether dislocations can transport hydrogen over large distances within a metal and how exactly hydrogen supersaturation can occur. The involvement of defects such as dislocations, is certainly important since strain rate is one of the important factors for HE. It has been observed that the time to HE failure in a 26Cr-1Mo alloy decreases with increasing peak strain rate, in the range of 10^{-10} to 10^{-7} sec^{-1} (167).

It is clear from the foregoing discussion that no single mechanism can account for HE. But it is to be pointed out that there are many similarities among various mechanisms. Ductile ruptures are expected from the pressure mechanism and also possibly from the dislocation (softening) mechanism. All other mechanisms predict brittle fracture due to hydrogen. The surface energy reduction mechanism and decohesion mechanism are very similar in that hydrogen reduces the metallic bond strength, but the locations of degradation are different. The decohesion mechanism is actually an improvement over the surface energy reduction mechanism, accounting for the specific embrittling nature of hydrogen versus other adsorbates. Since hydrogen degradation is proposed to occur inside the metallic bulk in the decohesion mechanism the possible rapid transport of hydrogen, versus any other species such as oxygen, will explain the special case of room temperature embrittlement by hydrogen. The decohesion mechanism has also a few similarities with the hydride mechanism in that the plasticity process is affected by the solid solution hydrogen in the former and the second phase hydride in the latter.

None of these phenomenological mechanisms directly bring out the important role played by impurities and stress state in the HE process. It is quite clear that extremely pure iron will not be hydrogen embrittled even at high hydrogen concentrations, but iron or its alloys will be hydrogen embrittled when impurities such as S, P, N, Si and Sn are present (22, 144, 168-172). HE of 26Cr-1Mo alloys has been found to be highly sensitive to the presence of small concentrations of interstitial elements, in particular nitrogen and carbon (173). Nitrogen segregated to grain boundaries or angular titanium carbo-nitrides near grain boundaries in this alloy, having high interstitial contents, enhance hydrogen absorption by trapping hydrogen at grain boundaries. Consequently, HE failure in the high interstitial 26Cr-1Mo alloy proceeds by an intergranular fracture process (173). In the low interstitial 26Cr-1Mo alloy, containing the stabilizer (to prevent sensitization and intergranular corrosion), niobium, in small concentration, HE seems to be caused by repeated formation and breakage of niobium hydrides under stress (173). There is also a parallelism in the role of impurities in HE with temper embrittlement behavior (170-172). However, the exact role of impurities and interaction of impurities with hydrogen to cause embrittlement in metallic systems is not understood. Stress state

36

also plays a prominent role in determining the extent of hydrogen embrittlement in nickel, steels, zirconium alloys and titanium (174-177). Ductility loss in Ni (174), the adverse effect of coarser grains in Ti (177), void link-up in Zr alloy (176), the amount of intergranular fracture in 4340 steel (175) due to hydrogen are all much more severe under equibiaxial tension than under plane strain which in turn is more severe than under uniaxial tension. Thus, hydrogen seems to augment the effect of stress state on plasticity, i.e., the decrease in the ductility of a metallic material going from a uniaxial tension state to a biaxial tension state is enhanced by hydrogen. In this respect, the thickness of the metal specimen plays an important role since thin specimens will be under the plane stress condition and thicker specimens will be under the more severe, plane strain condition. This is an important aspect to be considered in scaling the parametric values obtained in laboratory experiments on thin specimens for understanding HE behavior in real, thicker metallic systems.

DEDUCTIONS AND SUMMARY

It has been established that nascent hydrogen produced on a solid metallic material, by reduction of protons from an aqueous phase can affect the integrity of metallic materials in various ways, in particular the embrittlement fracture process. Since a majority of structural and industrial metallic members encounter some sort of an aqueous environment, the problem of hydrogen embrittlement is a serious concern to engineers and scientists. The involvement of electrical charges in the hydrogen discharge and sometimes also in the evolution processes means that the electrochemical nature of the reactions has to be carefully studied. To understand the hydrogen absorption and adsorption characteristics in a quantitative manner, from simple electropermeation measurements, transient and steady state permeation models are available. For a complete analysis of the kinetics, transport and mechanistic characteristics of hydrogen discharge, recombination and permeation processes, the following procedure is prescribed.

Set up a Devanathan Stachurski electropermeation apparatus. Prepare specimens of the metal/alloy to be tested in the form of a thin membrane. High purity specimens have to be used for understanding the transport behavior, while avoiding complications due to trapping. Specimen

thickness can range from 5 to 10 times the grain diameter to about 1000 times the square-root of hydrogen diffusivity, for performing a complete analysis including the film analysis. The specimen area exposed to the catholyte and anolyte should be more than 80 times the square of the specimen thickness, in order to reduce transverse leakage of hydrogen to less than 5%. The catholyte and anolyte have to be prepared carefully from high purity reagents and they have to be preelectrolyzed in bubbling nitrogen for removing impurities and dissolved oxygen to very low levels. After coating the anodic side with palladium, the anolyte can be introduced into the cell and a sufficient anodic potential applied. The background current density should be allowed to decay to values lower than $1 \mu A/cm^2$. Then, introduce the catholyte, simultaneously applying a high cathodic potential or cathodic current. The high cathodic potential (or current) should be below the critical cathodic potential (or current) at which irreversible damage can occur. Measure the cathodic electrode potential, cathodic current and anodic (permeation + background) current continuously. Analyze the transient permeation curve to obtain approximate values of the transport and trapping parameters. Verify the value of the transport parameter by independent methods.

Monitor the steady state cathodic current, cathodic electrode potential and permeation current. Conduct these tests for membranes of various thicknesses. Perform a film analysis (using the composite I-P-Z model) to gage the presence and role of surface films, if any. Also, obtain the values of the various kinetic parameters, surface coverages, α, etc. using appropriate models. These analyses will help to pinpoint the mechanism. Carry out the set of permeation experiments at different temperatures near room temperature, taking adequate precautions for the shift in the reference potentials and guarding against any other possible reactions. Obtain the activation energies of hydrogen absorption and adsorption and check their values by independent techniques. Determinations of transport parameters, surface coverages and activation energies by other experimental techniques will provide a means of independently validating the values obtained from the electropermeation technique and appropriate models.

In order to assess the effect of impurities or alloying elements in the material and species such as poisons in the catholyte, controlled additions can be done. Then, hydrogen permeation

38

characteristics, mechanism and trapping characteristics can be assessed with careful measurements and appropriate application of the models. A relationship such as $(k'')^{-1} = (k_{ads}/k_{abs}) + (D_l/k_{abs})(L)^{-1}$ can serve as a scaling parameter for transferring kinetic and related values obtained on thin specimens to thicker metallic specimens or members.

It is much harder to assess the effect of stress on HE. One can use stressed membranes in the electropermeation set-up with appropriate modifications such as used by Scully *et al* (143). Here, geometrical effects have to be carefully studied for meaningful interpretation. Also, stress/strain state effects are very important since thin specimens will be under the plane stress condition, while thicker specimens will be under the more severe plane strain condition. Therefore, appropriate scaling parameters have to be developed by emphasizing the fracture mechanics aspects.

A physical model is needed for understanding the hydrogen embrittlement mechanism, incorporating the features of hydrogen, stress, strain, strain rate, impurities and defects. The overwhelming effect of impurities on HE has to be properly addressed for a more general mechanism. It is not clear whether the primary function of impurities is to provide physical trapping sites for hydrogen or to modify locally the strain fields for interaction with hydrogen. It is possible that the locally modified strain fields can themselves enhance dynamic trapping of hydrogen, or, defects such as vacancies, interstitials and dislocations that carry the strain fields can be pinned locally by hydrogen. However, it seems inconceivable that hydrogen atoms can solely and effectively pin moving dislocations or vacancies. On the other hand, it is conceivable that impurity (or interstitial) atoms can kinetically arrest the motion of these defects, whereby many hydrogen atoms collect at these high energy sites. Accumulation of hydrogen at these kinetically arrested defects can, in turn, lower sufficiently the chemical potential of these defects to immobilize them at that particular location.

For example, if a cluster of vacancies are immobilized by the combined action of impurities and hydrogen, eventually molecular hydrogen can form within a coalescence of vacancies, i.e., a void. Moving dislocations can repeatedly annihilate a part of the void causing a reduction in void volume and thus increase the internal pressure due to the trapped hydrogen molecules in the void. Instead of a molecular hydrogen formation, one can envision formation of a metastable second phase of hydrogen

with the metal atoms, facilitated by the combined action of impurities and defects. The subsequent fracture process will be similar to the brittle hydride cracking mechanism. Another example is a set of moving dislocations being kinetically arrested by impurities and immobilized by hydrogen. This can lead to a reduction of the local plasticity and cause hardening. But if a number of vacancies are in motion (due to stress gradients), they can annihilate or unpin some of the locally immobilized dislocations. This can result in an enhancement of the local plasticity and cause softening. A cracking process can be initiated as a result of repeated (localized) softening and harde ng.

By carefully varying impurity concentration, dislocation density and vacancy concentration, the various aspects mentioned can be critically analyzed using the hydrogen permeation technique and models for metallic systems in aqueous environments. Finally, we can gain a complete understanding of hydrogen embrittlement only when we can reason why it does not occur in a host of metallic systems such as platinum and gold.

REFERENCES

1. Hudgins, C. M. 1969. *Materials Protection* 8: 41-

2. Oriani, R. A. 1969. *Proc. Conf. Fundamental Aspects of Stress Corrosion Cracking, Ohio State University, 1967*, ed. R. W. Staehle, A.J. Forty and D. vanRooyen, Houston: Natl. Assoc. Corros. Eng., pp.32-50.

3. Shanabarger, M. R. 1975. *Surf. Sci.* 52: 689-96.

4. Shanabarger, M. R. 1981. *Proc. Conf. Hydrogen Effects in Metals, 1980*, ed. I. M. Bernstein and A. W. Thompson, Warrendale: The Metall. Soc. AIME, pp. 135-41.

5. Johnson, H. H. 1988. *Metall. Trans.* 19A: 2371-87.

6. Nelson, H. G., Williams, D. P., Tetelman, A. S. 1971. *Metall. Trans.* 2: 953-59.

7. Hancock, G. G., Johnson, H. H. 1966. *Trans. Metall. Soc., AIME* 236: 513-16.

8. Johnson, H. H. 1977. *Proc. Conf. Stress Corrosion Cracking and Hydrogen Embrittlement of Iron Base Alloys, 1973, Unieux-Firminy, France,1973*, ed. R. W. Staehle and J. Hochmann, Houston: Natl. Assoc. Corros. Eng., pp. 382-89.

9. Smialowski, M. 1962. *Hydrogen In Steel*, Oxford: Pergamon. 452p.

10. Norton, F. J. 1953. *J. Appl. Phys.* 24: 499-

11. Shanabarger, M. R. 1974. *Surface Science* 44: 297-300.

12. Hogan, A. M., King, D. A. 1972. In *Adsorption-Desorption Phenomena*, ed. F. Ricca, Academic Press, New York, p. 329.

13. Frauenfelder, R. 1968. *J. Chem. Phys.* 48(9): 3955-65.

14. Johnson, D. L., Nelson, H. G. 1973. *Metall. Trans.* 47: 569-73.

15. Bond, A. P., Dundas, H. J. 1977. *Proc. Conf. Stress Corrosion and Hydrogen Embrittlement of Iron Base Alloys, 1973*, ed. R. W. Staehle and J. Hochmann, Houston: Natl. Assoc. Cor. Eng., pp. 1136-48.

16. Uhlig, H. H., Newberg, R. T. 1972. *Corrosion* 28: 337-39.

17. Bockris, J. O'M., Reddy, A. K. N. 1970. *Modern Electrochemistry, Vol. 2*, Plenum Press, New York, pp. 1231-38, 1261-62, 1333.

18. Conway, B. E. 1965. *Electrode Processes*, Ronald Press, New York, pp. 10, 14-16, 136-69.

19. Parsons, R. 1954. In *Modern Aspects of Electrochemistry, Vol. 1*, ed. J. O'M. Bockris, B. E. Conway, Academic Press, New York, Ch. 2.

20. Bockris, J. O'M., Devanathan, M. A., Muller, K. 1963. *Proc. Roy. Soc., London* A274: 55-

21. Bernstein, I. M. 1970. *Metall. Trans.* 1: 3143-50.

22. Oriani, R. A. 1978. *Ann. Rev. Mater. Sci.* 8: 327-57.

23. Tafel, J. 1905. *Z. Phys. Chem.* 50: 641-

24. Volmer, M., Wick, . 1935. *Z. Phys. Chem.* 172:429-

25. Horiuti, J., Ikusima, M. 1939. *Proc. Imp. Acad. Tokyo*, Japan 15: 39-

26. Frumkin, A. N., Slygin, A., 1953. *Acta Physicochim.* URSS 3: 791-

27. Vetter, K. J. 1967. *Electrochemical Kinetics*, Academic Press, London, pp. 516-40.

28. Bockris, J. O'M., McBreen, J., Nanis, L. 1965. *J. Electrochem. Soc.* 112(10): 1025-31.

29. Dafft, E. G., Bohnenkamp, K., Engell, H. J. 1979. *Cor. Sci.* 19: 591-612.

30. McBreen, J., Genshaw, M. A. 1969. See Ref. 2, pp. 51-63

31. Enyo, M. 1983. In *Comprehensive Treatise of Electrochemistry, Vol. 7*, Plenum Press, New York, pp. 241-300.

32. Daynes, H. 1920. *Proc. Roy. Soc.* A97: 286-

33. Frisch, H. L. 1957. *J. Phys. Chem.* 61: 93-95.

34. Devanathan, M. A. V., Stachurski, Z. 1964. *J. Electrochem. Soc.* 111: 619-23.

35. McNabb, A., Foster, P. K. 1963. *Trans. Metall. Soc. AIME* 227: 618-27.

36. Barrer, R. M. 1981. *Diffusion in and Through Solids*, Cambridge University Press, England, pp.

37. Nanis, L., Namboodhiri, T. K. G. 1972. *J. Electrochem. Soc.* 119(6): 691-94.

38. Quick, N. R., Johnson, H. H. 1978. *Acta Metall.* 26: 903-

39. Darken, L. S., Smith, R. P. 1949. *Corrosion* 5: 1-16.

40. Oriani, R. A. 1970. *Acta Metall.* 18: 147-57.

41. Hirth, J. P. 1980. *Metall. Trans.* 11A: 861-90.

42. Iyer, R. N., Pickering, H. W., Zamanzadeh, M. 1988. *Scripta Metall.* 22: 911-16.

43. Iyer, R. N., Pickering, H. W., Zamanzadeh, M. 1989. *J. Electrochem. Soc.* 136: 2463-70.

44. Bonhoeffer, K. F. 1924. *Z. Phys. Chem.* A113: 199-

45. Bockris, J. O'M., Khan, S. U. M. 1979. *Quantum Electrochemistry*, Plenum Press, New York, pp. 315-78.

46. Conway, B. E. 1959. *Can. J. Chem.* 37: 178-89.

47. Gileadi, E., Conway, B. E. 1964. In *Modern Aspects of Electrochemistry, No. 3*, Butterworths, Washington, pp. 347-443.

48. Conway, B. E., Bockris, J. O'M. 1957. *Can. J. Chem.* 35: 1124-36.

49. Conway, B. E., Salomon, M. 1964. *Ber. Bunsenges.* 68: 331-40.

50. Beeck, O. 1950. *Advan. Catalysis* 2: 151-95.

51. Germer, L. H., MacRae, A. U. 1962. *J. Chem. Phys.* 37: 1382-

52. Petch, N. J. 1956. *Philos. Mag.* 1(Ser.8): 331-37.

53. Kim, C. D., Wilde, B. E. 1971. *J. Electrochem. Soc.* 118: 202-06.

54. Pearson, , Buter, . 1938. *Trans. Faraday Soc.* 34: 1163-

55. Devanathan, M. A., Bockris, J. O'M., Mehl, W. 1959/60. *J. Electroanal. Chem.* 1: 143-60

56. Gerischer, H., Mehl, W. 1955. *Z. Elektrochem.* 59: 1049-

57. Bockris, J. O'M., Carbajal, J. L., Scharifker, B. R., Chandrasekaran, K. 1987. *J. Electrochem. Soc.* 134(8): 1957-63.

58. Ateya, B. G., Abd Elal, H. E. 1987. *Proc. Conf. Corrosion - Industrial Problems, Treatment and Control Techniques, Kuwait, 1984*, ed. V. Ashworth, KFAS Proceedings Series Vol. 2, pp. 201-22.

59. Sköld, K., Nelin, G. 1967. *J. Phys. Chem. Solids* 28: 2369-

60. Springer, T. 1972. *Springer Tracts in Modern Physics, Vol. 24*, Springer-Verlag, Berlin and New York, pp.

61. Gissler, W. 1972. *Ber. Bunsenges. Phys. Chem.* 76: 770-

62. Cotts, R. M. 1972. *Ber. Bunsenges. Phys. Chem.* 76: 760-

63. Sicking, G., Buchold, H. 1971. *Z. Naturforsch.* 26a: 1973-

64. Katz, L., Guinan, M., Borg, R. L. 1971. *Phys. Rev.* B4: 330-

65. Armacanqui, M. E., Oriani, R. A. 1987. *Mat. Sci. Eng.* 91: 143-52.

66. Armacanqui, M. E., Oriani, R. A. 1987. *Mat. Sci. Eng.* 92: 127-32.

67. Bockris, J. O'M., Subramanyan, P. K. 1971. *J. Electrochem. Soc.* 118: 1114-19.

68. Subramanyan, P. K. 1981. In *Comprehensive Treatise of Electrochemistry, Vol. 4*, Plenum Press, New York, pp. 411-62.

69. Fontana, M.G., 1986. Corrosion Engineering, McGraw-Hill, New York, p. 457.

70. Forchhammer, P., Engell, H. J. 1969. *Werkstoffe Und Korrosion.* 20: 1-12.

71. Kaesche, H. 1960. *Z. Physik. Chem.* N. F. 26: 138-

72. Kaesche, H. 1962. *Z. Physik. Chem.* N. F. 34: 87-108

73. Pickering, H. W., Frankenthal, R. P. 1972. *J. Electrochem. Soc.* 119: 1297-1304

74. Pickering, H. W. 1986. *Corrosion* 42: 125-40.

75. Pickering, H. W., Frankenthal, R. P. 1971. *Proc. Intern. Conf. Localized Corrosion, 1975*, ed. R. W. Staehle, B.F. Brown, G. Kruger and A. Agrawal, Houston, Texas: Natl. Assoc. Corros. Eng., pp. 261-69.

76. Oldfield, J. W., Lee, T. S., Kain, R. M. 1987. In *Corrosion Chemistry Within Pits, Crevices and Cracks*, ed. A. Turnbull, Her Majesty's Stationery Office, London, pp. 89-

77. Valdes, A., Pickering, H. W. (in press). *Proc. Intl. Conf. Localized Corrosion, 1987*, ed. H. S. Isaacs *et al*, Orlando, Florida.

78. Kelly, W. K., Iyer, R. N., Pickering, H. W., to be submitted to *Corrosion*.

79. Pickering, H. W. 1989. *Corrosion Sci.* 29: 325-41.

80. Chatterjee, S. S., Ateya, B. G., Pickering, H. W. 1978. *Metall. Trans.* 9A: 389-95.

81. Zamanzadeh, M., Allam, A., Pickering, H. W., Hubler, G. K. 1980. *J. Electrochem. Soc.* 127: 1688-93.

82. Pickering, H. W., Zamanzadeh, M. 1981. *Proc. Conf. Hydrogen Effects in Metals, 1980*, ed. I. M. Bernstein and A. W. Thompson, Warrendale: The Metall. Soc. AIME, pp. 143-52.

83. Zamanzadeh, M., Allam, A., Kato, C., Ateya, B.G., Pickering, H. W. 1982. *J. Electrochem. Soc.* 129: 284-89.

84. Wilde, B. E., Kim, C. D., Turn, J. C. Jr. 1982. *Corrosion* 38: 515-

85. Kato, C., Grabke, H. J., Egert, B., Panzner, G. 1984. *Corrosion Science* 24: 591-611.

86. Blanchard, P., Troiano, A. R. 1960. *Mem. Sci. Rev. Metall.* 57: 409-22.

87. Latanision, R. M., Operhauser, H. Jr. 1974. In *Hydrogen in Metals, 1973*, ed. I. M. Bernstein, A. W. Thompson, pp. 539-42. Metals Park, OH: Am. Soc. Met., pp. 539-42.

88. Speidel, M. O. 1974. See Ref. 87, pp. 249-71.

89. Patton, N. E., Williams, J. C. 1974. See Ref. 87, pp. 409-31.

90. Van Fossen, R. H. Jr., Scott, T. E., Carlson, O. N. 1965. *J. Less-Common Met.* 9: 437-51.

91. Magnani, N. J. 1976. In *Effect of Hydrogen on Behavior of Materials*, ed. A. W. Thompson, I. M. Bernstein, pp. 189-99. New York: Metall. Soc. AIME.

92. Birnbaum, H. K., Wadley, H. 1975. *Scripta Metall.* 9: 1113-16.

93. Gahr, S., Grossbeck, M. L., Birnbaum, H. K. 1977. *Acta Metall.* 25: 125-34.

94. Grossbeck, M. L., Birnbaum, H. K. 1977. *Acta Metall.* 25: 135-48.

95. Ingram, A. G., Bartlett, E. S., Ogden, H. R. 1963. *Trans. Metall. Soc. AIME* 227: 131-36.

96. Birnbaum, H. K., Grossbeck, M. 1974. See Ref. 87, pp. 303-23.

97. Seelinger, S., Stolloff, N. S. 1971. *Metall. Trans.* 2: 1481-84.

98. Johnson, H. R., Dini, J. W. 1974. See Ref. 70, pp. 325-43.

99. Devanathan, M. A. V., Stachurski, Z., Beck, W. 1963. *J. Electrochem. Soc.* 110: 886-890.

100. Crank, J. 1975. *Mathematics of Diffusion, 2nd ed.*, Clarendon Press, Oxford U., England, pp.

101. Powers, R. W. 1969. *Electrochem. Tech.* 2: 163-

102. Thomas, G. J. 1981. *Proc. Conf. Hydrogen Effects in Metals, 1980*, ed. I. M. Bernstein and A. W. Thompson, Warrendale: The Metall. Soc. AIME, pp. 77-85.

103. McBreen, J., Nanis, L., Beck, W. 1966. *J. Electrochem. Soc.* 113: 1218-22.

104. Boes, N., Zuchner, H. 1976. *J. Less-Common Metals* 49: 223-40.

105. Wicke, E., Brodowsky, H. 1978. *Topics in Applied Physics - Hydrogen in Metals II, Vol. 29*, Springer-Verlag, New York, NY, pp. 73-155.

106. Nanis, L., Namboodhiri, T. K. G. 1977. *Proc. Conf. Stress Corrosion Cracking and Hydrogen Embrittlement of Iron Base Alloys, Unieux-Firminy, France, 1973*, ed. R. W. Staehle and J. Hochman, Houston: Natl. Assoc. Corros. Eng., pp. 432-44.

107. Hirth, J. P., Johnson, H. H. 1976. *Corrosion* 32: 3-22.

108. Volkl, J., Alefeld, G. 1978. *Topics in Applied Physics - Hydrogen in Metals I, Vol. 28*, Springer-Verlag, New York, NY, pp. 321-48.

109. Wu, E. 1987. *J. Electrochem. Soc.* 134: 2126-33.

110. McKibbin, R., Harrington, D. A., Pound, B. G., Sharp, R. M., Wright, G. A. 1987. *Acta Met.* 35: 253-

111. Pound, B. G., Sharp, R. M., Wright, G. A. 1987. *Acta Met.* 35: 263-

112. Pound, B. G. 1989. Corrosion 45: 18-

113. Johnson, H. H., Lin, R. W. 1981. *Proc. Conf. Hydrogen Effects in Metals, 1980*, ed. I. M. Bernstein and A. W. Thompson, Warrendale: The Metall. Soc. AIME, pp. 3-25.

114. Wert, C. A. 1978. *Topics in Applied Physics - Hydrogen in Metals II, Vol. 29*, Springer-Verlag, New York, NY, pp. 305-30.

115. Schaumann, G., Volkl, J., Alefeld, G. 1968. *Phys. Rev. Lett.* 21: 891-

116. Coehn, A., Jurgens, H. 1931. *Z. Phys.* 71: 179-

117. Kronmuller, H. 1970. *Vacancies and Interstitials in Metals*, North-Holland Publication, Amsterdam, Holland, pp. 667-

118. Cotts, R. M. 1978. *Topics in Applied Physics - Hydrogen in Metals I, Vol. 28*, Springer-Verlag, New York, NY, pp. 227-65.

119. Wagner, F. E., Wortmann, G. 1978. *Topics in Applied Physics - Hydrogen in Metals I, Vol. 28*, Springer-Verlag, New York, NY, pp. 131-67.

120. Skold, K. 1978. *Topics in Applied Physics - Hydrogen in Metals I, Vol. 28*, Springer-Verlag, New York, NY, pp. 267-87.

121. Devanathan, M. A. V., Selvaratnam, M. 1960. *Trans. Faraday Soc.* 56: 1820-1831.

122. Flitt, H., Bockris, J. O'M. 1982. *Int. J. Hydrogen Energy* 7: 411-

123. Iyer, R. N., Pickering, H. W. (in preparation).

124. Brunauer, S., Emmett, P. H., Teller, E. 1938. *J. Am. Chem. Soc.* 60: 309-

125. Emmett, P. H., Brunauer, S. 1937. *J. Am. Chem. Soc.* 59: 1553- , 2682-

126. Kawashima, A. Hashimoto, K., Shimodaira, S. 1976. *Corrosion* 32: 321-

127. Sury, P. 1976. *Corr. Sci.* 16: 879-901.

128. Hashimoto, M., Sato, E., Murata, T. 1980. *Proc. Conf. Hydrogen in Metals, 1979, JIMIS-2*, Japan: Trans. Japan Inst. Met., pp. 209-11.

129. Berkowitz, B. J., Horowitz, H. H. 1982. *J. Electrochem. Soc.* 129: 468-74.

130. Iofa, Z. A., Kam, F. L. 1974. *Protection of Metals* 10: 12-

131. Boucher, B. E. 1969. *Proc. Fourth Int. Cong. on Met. Corr., 196?*, ed. , Houston: Natl. Assoc. Corros. Eng., pp. 550-

132. Bolmer, P. W. 1965. *Corrosion* 21: 69-

133. Iyer, R. N., Takeuchi, I., Zamanzadeh, M., Pickering, H. W. *Corrosion* , in press.

134. Murayama, H. Sakashita, M., Sato, N. 1980. *Proc. Conf. Hydrogen in Metals, 1979, JIMIS-2*, Japan: Trans. Japan Inst. Met., pp. 297-300.

135. Iyer, R. N., Takeuchi, I., Zamanzadeh, M., Pickering, H. W. (in preparation).

136. Wilhelm, S. M., Vera, J., Hackerman, N. 1983. *J. Electrochem. Soc.* 130: 2129-32.

137. Ash, R., Barrer, R. M., Palmer, D. G. 1965. *Br. J. Appl. Physics* 16: 873-

138. Roehrig, H. D., Hecker, R., Blumensaat, J. Schefer, J. 1975. *Nucl. Eng. Design* 34: 157-

139. Sukhotin, A. M., Sapelova, E. V., Reingeverts, M. D. 1985. *Corr. Sci.* 25: 93-

140. Pyun, S. I., Oriani, R. A. 1989. *Corr. Sci.* 29: 485-96.

141. Habib, M., Bockris, J. O'M. In *Comprehensive Treatise of Electrochemistry, Vol. 4,* Plenum Press, New York, NY, pp. 135-219.

142. Iyer, R. N., Pickering, H. W. (in preparation).

143. Scully, J. R., Moran, P. J. 1988. *J. Electrochem. Soc.* 135: 1337-48.

144. Nelson, H. G. 1983. *Treatise on Materials Sci. and Tech., Vol. 25 - Embrittlement of Eng. Alloys,* ed. C. L. Briant and S. K. Banerji, Academic Press, New York, NY, pp. 275-359.

145. Gahr, S., Makenas, B. J., Birnbaum, H. K. 1980. *Acta Met.* 28: 1207-13.

146. Ciaraldi, S. W., Nelson, J. L., Yeske, R. A., Pugh, E. N. 1981. *Proc. Conf. Hydrogen Effects in Metals, 1980,* ed. I. M. Bernstein and A. W. Thompson, Warrendale: The Metall. Soc. AIME, pp. 437-47.

147. Westlake, D. G. 1969. *Trans. ASM* 62: 1000-

148. Birnbaum, H. K. 1980. *Environment Sensitive Fracture Mechanisms, ?,* ed. Z. A. Foroulis, Warrendale: AIME, pp. 326-60.

149. Zapffe, C., Sims, C. 1941. *Trans. AIME* 145: 225-

150. Christmann, K., Schober, O., Ertl, E., Newmann, M. 1974. *J. Chem. Phys.* 60: 4528-

151. Barnett, W. J., Troiano, A. R. 1957. *J. Met. Trans. AIME* 209: 486-94.

152. Oriani, R. A. 1972. *Ber. Bunsenges. Phys. Chem.* 76: 848-57.

153. Oriani, R. A. 1977. *Proc. Conf. Stress Corrosion Cracking and Hydrogen Embrittlement of Iron Base Alloys, Unieux-Firminy, France, 1973*, ed. R. W. Staehle *et al.*, Houston: Natl. Assoc. Corros. Eng., pp. 351-58.

154. Troiano, A. R. 1960. *Trans. ASM* 52: 54-80.

155. Beachem, C. D. 1972. *Metall. Trans.* 3: 437-51.

156. Louthan, M. R., Jr., Cuskey, G. R., Jr., Donovan, J. A., Rawl, D. E. 1972. *J. Mat. Sci. Eng.* 10: 357-

157. Windle, R. H., Smith, G. C. 1970. *Met. Sci. J.* 4: 136-

158. Bastien, P., Azou, P. 1951. *C. R. Acad. Sci. Paris* 232: 1845-48.

159. Tien, J. K., Thompson, A. W., Bernstein, I. M., Richards, R. J. 1976. *Metall. Trans.* 7A: 821-29.

160. Johnson, H. H., Hirth, J. P. 1976. *Metall. Trans.* 7A: 1543-48.

161. Matsumoto, T., Eastman, J., Birnbaum, H. K. 1981. *Scripta Met.* 15: 1033-37.

162. Eastman, J., Heubaum, F., Matsumoto, T., Birnbaum, H. K. 1982. *Acta Met.* 30: 1579-86.

163. Xie, S. X., Hirth, J. P. 1983. *Mat. Sci. Eng.* 60: 207-12.

164. Tabata, T., Birnbaum, H. K. 1983. *Scripta Met.* 17: 947-50.

165. Kimura, H., Matsui, H., Kimura, A., Kimura, T., Oguri, K. 1981. *Proc. Conf. Hydrogen Effects in Metals, 1980*, ed. I. M. Bernstein and A. W. Thompson, Warrendale: The Metall. Soc. AIME, pp. 191-208.

166. Tabata, T., Birnbaum, H. K. 1984. *Scripta Met.* 18: 231-36.

167. Iyer, R. N., Hehemann, R. F. 1990. *Proc. Int. Conf. Environment-Induced Cracking of Metals, 1988, Kohler, Wisconsin*, ed. M. B. Ives and R. P. Gangloff, ASM-NACE-TMS (in press).

168. Rath, B. B., Bernstein, I. M. 1971. *Metall. Trans.* 2: 2845-51.

169. Cornet, M., Raczynski, W., Talbot-Besnard, S. 1972. *Mem. Sci. Rev. Metall.* 69: 27-32.

170. Viswanathan, R. Hudak, S. J., Jr. 1977. *Metall. Trans.* 8A: 1633-37.

171. McMahon, C. J., Jr., Briant, C. L., Banerji, S. K. 1977. *Conf. Proc. Fracture 1977,* Waterloo: Canada 1: 363-85.

172. Banerji, S. K., McMahon, C. J., Jr., Feng, H. C. 1978. Metall. Trans. 9A: 237-47.

173. Iyer, R. N., Hehemann, R. F., Troiano, A. R. 1990. *Environmentally Assisted Cracking: Science and Eng., ASTM STP 1049,* ed. W. B. Lisagor, T. W. Crooker, B. N. Leis, Philadelphia: Am. Soc. Testing and Materials, pp. 30-41.

174. Kampe, S. L., Koss, D. A. 1986. *Acta Met.* 34: 55-61.

175. Louthan, M. R., Jr., Sisson, R. D., Jr., McNitt, R. P., Smith, P. E. 1981. *Proc. Conf. Hydrogen Effects in Metals, 1980,* ed. I. M. Bernstein and A. W. Thompson, Warrendale: The Metall. Soc. AIME, pp. 829-50.

176. Yunchang, F., Koss, D. A. 1985. *Scripta Met.* 19: 675-81.

177. Gerard, D. A., Koss, D. A. 1985. Scripta Met. 19: 1521-24.

(A) Film-free Metal $(\lambda=0)$ (B) Filmed Metal $(\lambda \ll L)$ (C) Filmed Metal $(\lambda \sim L)$
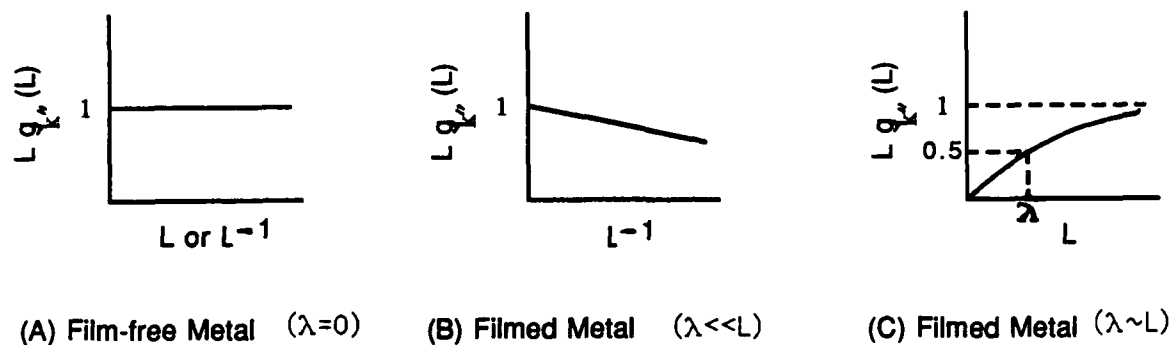
Figure 1: Schematic of film effect on $L\,g_{k''}(L)$ versus L or L^{-1} plots.

(A) Bulk diffusion control   (B) Interface control   (C) Mixed control

(D) Film diffusion control   (E) Film-solution interface control
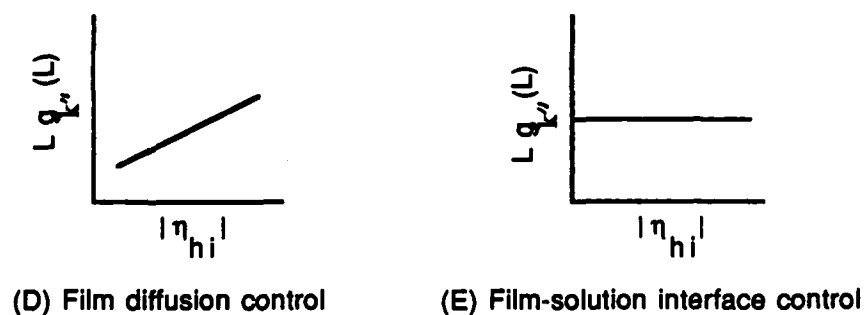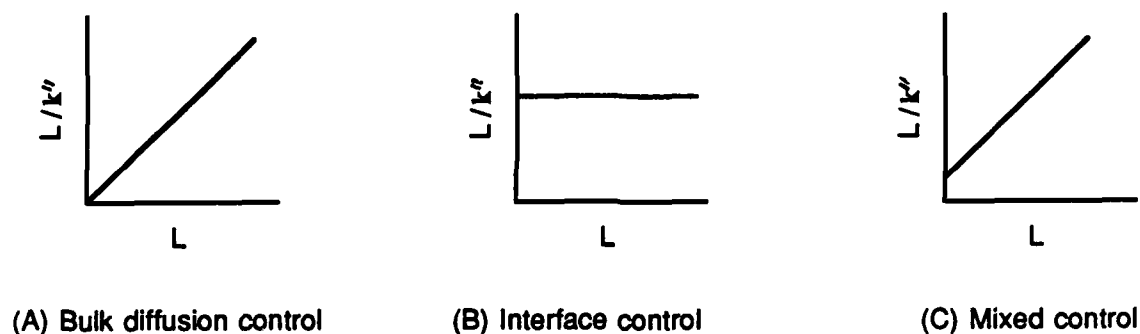
Figure 2: Schematic of various cases of transport and kinetic control.

BASIC DISTRIBUTION LIST

Technical and Summary Reports   1988

Organization	Copies	Organization	Copies
Defense Documentation Center Camerson Station Alexandria, VA 22314	12	Naval Air Prop. Test Ctr.. Trenton, NY 08628 ATTN: Library	1
Office of Naval Research Dept. of the Navy 800 N. Quincy Street Arlington, VA 22217 Attn: Code 1131	3	Naval Contruction Battallion Civil Engineering Laboratory Port Hueneme, CA 93043 ATTN: Materials Div.	1
Naval Research Laboratory Washington, DC 20375 ATTN: Codes 6000 6300 2627		Naval Electronics Laboratory San Diego, CA 92152 ATTN: Electron Materials Sciences Division	1
Naval Air Development Center Code 606 Warminister, PA 18974 ATTN: Dr. J. DeLuccia		Naval Missile Center Materials Consultant Code 3312-1 Point Mugu, CA 92041	1
Commanding Officer Naval Surface Weapons Center White Oak Laboratory Silver Spring, MD 20910 ATTN: Library	1	Commander David Taylor Research Center Bethesda, MD 20084	1
Naval Oceans Systems Center San Diego, CA 92132 ATTN: Library	1	Naval Underwater System Ctr. Newport, RI 02840 ATTN: Library	1
Naval Postgraduate School Monterey, CA 93940 ATTN: Mechanical Engineering Department	1	Naval Weapons Center China Lake, CA 93555 ATTN: Library	1
Naval Air Systems Command Washington, DC 20360 Attn: Code 310A Code 5304B Code 931A	1 1 1	NASA Lewis Research Center 21000 Brookpark Road Cleveland, OH 44135 ATTN: Library	1
Naval Sea System Command Washington, DC 20362 ATTN: Code 05M Code 05R	1 1	National Bureau of Standards Gaithersburg, MD 20899 Attn: Metallurgy Division Ceramics Division Fracture & Deformation Division	1 1 1

Naval Facilities Engineering Command Alexandria, VA 22331 ATTN: Code 03 1	Defense Metals & Ceramics Information Center Battelle Memorial Inst. 505 King Avenue Columbus, OH 43201 1

Naval Facilities Engineering
 Command
Alexandria, VA 22331
ATTN: Code 03   1

Defense Metals & Ceramics
 Information Center
Battelle Memorial Inst.
505 King Avenue
Columbus, OH 43201   1

Scientific Advisor
Commandant of the Marine Corps
Washington, DC 20380
ATTN: Code AX   1

Metals and Ceramics Div.
Oak Ridge National Laboratory
P.O. Box X
Oak Ridge, TN 37380   1

Army Research Office
P.O. Box 12211
Research Triangle Park, NC 27709
ATTN: Metallurgy & Ceramics
            Program   1

Los Alamos Scientific Lab.
P.O. Box 1663
Los Alamos, NM 87544
ATTN: Report Librarian   1

Army Materials and Mechanics
 Research Center
Watertown, MA 02172
ATTN: Research Programs Office   1

Argonne National Laboratory
Metallurgy Division
P.O. Box 229
Lemont, IL 60439   1

Air Force Office of Scientific
 Research/NE
Building 410
Bolling Air Force Base
Washington, DC 20332
ATTN: Electronics & Materials
            Science Directorate   1

Brookhaven National Laboratory
Technical Information Division
Upton, Long Island
New York 11973
Attn: Research Library   1

Lawrence Radiation Lab.
Library
Building 50, Room 134
Berkely, CA   1

NASA Headquarters
Washington, DC 20546
Attn: Code RM   1

David Taylor Research Ctr
Annapolis, MD 21402-5067
ATTN: Code 281   1
            Code 2813   1
            Code 0115   1

RE/1131/88/75

4315 (036)

<u>Supplemental Distribution List</u>   Feb 1988

Prof. I.M. Bernstein
Illinois Institute of Technology
IIT Center
Chicago, Ill 60615

Prof. H.K. Birnbaum
Dept. of Metallurgy & Mining Eng.
University of Illinois
Urbana, Ill 61801

Prof. H.W. Pickering
Dept. of Materials Science and Eng.
The Pennsylvania State University
University Park, PA 16802

Prof. D.J. Duquette
Dept. of Metallurgical Eng.
Rensselaer Polytechnic Inst.
Troy, NY 12181

Prof. J.P. Hirth
Dept. of Metallurgical Eng.
The Ohio State University
116 West 19th Avenue
Columbus, OH 43210-1179

Prof. H. Leidheiser, Jr.
Center for Coatings and Surface Research
Sinclair Laboratory, Bld. No. 7
Lehigh University
Bethlehem, PA 18015

Dr. M. Kendig
Rockwell International Science Center
1049 Camino Dos Rios
P.O. Box 1085
Thousand Oaks, CA 91360

Prof. R. A. Rapp
Dept. of Metallurgical Eng.
The Ohio State University
116 West 19th Avenue
Columbus, OH 43210-1179

Profs. G.H. Meier and F.S.Pettit
Dept. of Metallurgical and
Materials Eng.
University of Pittsburgh
Pittsburgh, PA 15261

Dr. W. C. Moshier
Martin Marietta Laboratories
1450 South Rolling Rd.
Baltimore, MD 21227-3898

Prof. P.J. Moran
Dept. of Materials Science & Eng.
The Johns Hopkins University
Baltimore, MD 21218

Prof. J. Kruger
Dept. of Materials Science & Eng.
The Johns Hopkins University
Baltimore, MD 21218

Prof. R.P. Wei
Dept. of Mechanical Engineering
and Mechanics
Lehigh University
Bethlehem, PA 18015

Prof. W.H. Hartt
Department of Ocean Engineering
Florida Atlantic University
Boca Raton, Florida 33431

Dr. B.G. Pound
SRI International
333 Ravenswood Ave.
Menlo Park, CA 94025

Prof. C.R. Clayton
Department of Materials Science
& Engineering
State University of New York
Stony Brook
Long Island, New York 11794

Prof. Boris D. Cahan
Dept. of Chemistry
Case Western Reserve Univ.
Cleveland, Ohio 44106

Dr. K. Sadananda
Code 6323
Naval Research Laboratory
Washington, D.C. 20375

Prof. M.E. Orazem
Dept. of Chemical Engineering
University of Virginia
Charlottesville, VA 22901

Dr. G.R. Yoder
Code 6384
Naval Research Laboratory
Washington, D.C. 20375

Dr. N. S. Bornstein
United Technologies Research Center
East Hartford, CT 06108

Dr. A.L. Moran
Code 2812
David Taylor Research Center
Annapolis, MD 21402-5067

Dr. B.E. Wilde
Dept. of Metallurgical Engineering
The Ohio State University
116 West 19th Avenue
Columbus, OH 43210-1179

Prof. G.R. St. Pierre
Dept. of Metallurgical Eng.
The Ohio State University
116 West 19th Avenue
Columbus, OH 43210-1179

Prof. G. Simkovich
Dept. of Materials Science & Eng.
The Pennsylvania State University
University Park, PA 16802

Dr. E. McCafferty
Code 6322
Naval Research Laboratory
Washington, D. C. 20375

Dr. J.A. Sprague
Code 4672
Naval Research Laboratory
Washington, D.C. 20375

Dr. C.M. Gilmore
The George Washington University
School of Engineering & Applied
 Science
Washington, D.C. 20052

Dr. F.B. Mansfeld
Dept. of Materials Science
University of Southern California
University Park
Los Angeles, CA 90089

Dr. Ulrich Stimming
Dept. of Chemical Eng. & Applied
 Chemistry
Columbia University
New York, N.Y. 10027

Prof. J. O'M. Bockris
Dept. of Chemistry
Texas A & M University
College Station, TX 77843